SOLAR HEATING & COOLING PROGRAMME
INTERNATIONAL ENERGY AGENCY

Development and Characterization of Improved Thermochemical Materials

IEA SHC TASK 58 / ES Annex 33 | “Material Development for Compact Thermal Energy Storage”

Technology Collaboration Programme
by iea

Development and Characterization of Improved Thermochemical Materials

This is a report from SHC Task 58 / ES Annex 33: | “Material Development for Compact Thermal Energy Storage”

Subtask DT2:

Development and Characterization of Improved Thermochemical Materials

Alenka Ristić, National Institute of Chemistry, Slovenia
July 2021
Report number DT2, DOI: 10.18777/ieashc-task58-2024-0001

Solar Heating and Cooling Technology Collaboration Programme (IEA SHC)

The Solar Heating and Cooling Technology Collaboration Programme was founded in 1977 as one of the first multilateral technology initiatives ("Implementing Agreements") of the International Energy Agency.

Our mission is *"Through multi-disciplinary international collaborative research and knowledge exchange, as well as market and policy recommendations, the IEA SHC will work to increase the deployment rate of solar heating and cooling systems by breaking down the technical and non-technical barriers."*

IEA SHC members carry out cooperative research, development, demonstrations, and exchanges of information through Tasks (projects) on solar heating and cooling components and systems and their application to advance the deployment and research and development activities in the field of solar heating and cooling.

Our focus areas, with the associated Tasks in parenthesis, include:

- Solar Space Heating and Water Heating (Tasks 14, 19, 26, 44, 54)
- Solar Cooling (Tasks 25, 38, 48, 53, 65)
- Solar Heat for Industrial and Agricultural Processes (Tasks 29, 33, 49, 62, 64)
- Solar District Heating (Tasks 7, 45, 55)
- Solar Buildings/Architecture/Urban Planning (Tasks 8, 11, 12, 13, 20, 22, 23, 28, 37, 40, 41, 47, 51, 52, 56, 59, 63, 66)
- Solar Thermal & PV (Tasks 16, 35, 60)
- Daylighting/Lighting (Tasks 21, 31, 50, 61)
- Materials/Components for Solar Heating and Cooling (Tasks 2, 3, 6, 10, 18, 27, 39)
- Standards, Certification, and Test Methods (Tasks 14, 24, 34, 43, 57)
- Resource Assessment (Tasks 1, 4, 5, 9, 17, 36, 46)
- Storage of Solar Heat (Tasks 7, 32, 42, 58)

In addition to our Task work, other activities of the IEA SHC include our:

- SHC Solar Academy
- *Solar Heat Worldwide*, annual statics report
- SHC International Conference

Our members

Australia	European Copper Institute	Slovakia
Austria	France	South Africa
Belgium	Germany	Spain
Canada	International Solar Energy Society	Sweden
CCREEE	Italy	Switzerland
China	Netherlands	Turkey
Denmark	Norway	United Kingdom
EACREEE	Portugal	
ECREEE	RCREEE	
European Commission	SACREEE	

For more information on the IEA SHC work, including many free publications, please visit www.iea-shc.org.

Contents

Contents .....

1 Development and Characterization of Improved Thermochemical Materials **1**

1.1 Introduction 1

1.2 Development and identification of the novel chemical reactions and composite materials 1

1.3 Definition of the relevant material parameters 2

1.4 Characterization of novel reactions and materials by material properties 2

1.4.1 Sorption materials 2

1.4.2 Chemical reaction 15

1.4.3 Overview of TCM materials 33

1.5 Developement of the TCM material databases implemented in Task42/Annex 29 35

1.5.1 Material parameters for the chemical reaction database using K_2CO_3*1.5 H_2O as an example: ... 35

1.5.2 Material parameters for the sorption materials database 38

1.6 Acknowledgements 38

1 Development and Characterization of Improved Thermochemical Materials

1.1 Introduction

The Subtask 2T focuses on the development of improved TCM materials, which are based on sorption (micro/mesoporous solids and liquids (hydroxides)), chemical reactions (salt hydrates and metal oxides/hydroxides) and combinations (zeolites / graphite + salt hydrates / metal). The activities of the Subtask 2T include the listing of new and improved existing materials, determination of material properties, measurement of thermo-physical properties and expanding the database implemented within the previous task.

One of the goals is to determine the differential heat of sorption / reaction of TCM materials, which can be expressed as a characteristic curve in order to derive possible storage performance.

This Working Group 2T includes the following activities:

1) Develop and identify novel chemical reactions and composite materials
2) Define relevant material parameters
3) Characterize novel reactions and materials by material properties
4) Maintenance and expansion of the materials database implemented in Task42/Annex 29

In the framework of the Task/Annex 58/33 (IEA, TCPs ES/SHC 2017-2019), significant R&D effort was directed toward the development of new or improved TES materials. TCM used for thermal energy storage are an important class of materials which substantially contribute to the efficient use and conservation of waste heat and solar energy and lead to low carbon society. Comparing to the previous task the number of TCM groups increased significantely. Detailed information on R&D of compact TCM materials is presented in **section 3.**

1.2 Development and identification of the novel chemical reactions and composite materials

Development of TCM materials has been devoted to characterization of new and improved TCM materials as powders: chemical reactants and sorption materials and composites as well as liquids. Novel chemical reactions and composite materials were developed and identified. Water and ammonia were used in chemical reactions, while only water was used for sorption materials. Table 1 presents different types of TCM materials, based on the following mechanism: adsorption, chemical reactions, absorption and mixture of all three mechanisms, investigated during the last 3 years.

Table 1: Different TCMs developed at the joint Task/Annex 58/33 from 2017 to 2019

Sorption materials	Chemical reactions	Composites	Liquids
MOFs: MIL-160, MIL-101, MIL-125,	$CuCl_2$-H_2O, $MgCl_2$-H_2O LiCl-H_2O, $CaCl_2$-H_2O $LaCl_2$	SAPO-34/Al	LiCl
Zeolites: 13X binder-free (BF) and with binder, YBF, deaYBF, Y with binder, 4A with binder and BF	$SrBr_2$-H_2O $MgBr_2$-H_2O	$Mg(OH)_2$-EG (expanded graphite), $Mg(OH)_2$-CNT (carbon nanotube)	LiBr
Aluminophosphates: APO-LTA, APO-34, APO-18, FAPO-34, SAPO-34, FAM-Z02, APO-5	K_2CO_3-H_2O	$MgCl_2$-silica gel $CaCl_2$-silica gel $SrBr_2$-silica gel	NaOH
Porous SiC foam	MgO-$Mg(OH)_2$ CTABr-$Mg(OH)_2$	$SrBr_2$-graphite	$ZnCl_2$

	Ca/MgO-Ca/$Mg(OH)_2$, Co/MgO-Co/$Mg(OH)_2$, Ni/MgO-Ni/$Mg(OH)_2$,		
Silica gel	CaO/$Ca(OH)_2$,	LiCl-vermiculite, clinoptilolite	
	Fe/$CaMnO_3$, $CaMnO_3$ Copper oxides Iron oxides (redox reaction)	HKUST-1, CAU-10, MIL-100, Al-fumarate, SAPO-34-Al_2O_3 foam HKUST-1, CAU-10, MIL-101, UiO-66-ceramic foam HKUST-1, CAU-10-SiC foam CAU-10, MIL-100, Al-fumarate-Al foam	
	Li_2SO_4/Na_2SO_4	Ca/Mg/LiX-Al_2O_3 foam Ca/Mg/LiX-ceramic cellular foams	
	LiOH/LiBr	$CaCl_2$-PHTS, SG, vermiculite, clinoptilolite	
	$NiCl_2$, $CoCl_2$, $FeCl_3$, $CuCl_2$-NH_3	$SrCl_2$-ENG-NH_3	
	$MgCl_2$, $SrCl_2$-NH_3	$MgSO_4$-silicone foam	
	$CoSO_4$, $FeSO_4$, $CuSO_4$-NH_3		
	$Ba(OH)_2$-H_2O		
	Na_2SO_4, Na_2S		
	Ettringite ($Ca_6Al_2(SO_4)_3(OH)_{12}\cdot 26H_2O$)		
	$CuCaYCl_2$, $Ca_xTi_yCu_2Cl_2$ -NH_3		
	$CaCl_2$-attapulgite/cellulose		

1.3 Definition of the relevant material parameters

Relevant material parameters were defined and incorporated into two databases based on chemical reactions and adsorption of gas on solids, respectively. See overviews of the databases in **section 4**.

1.4 Characterization of novel reactions and materials by material properties

1.4.1 Sorption materials

1.4.1.1 National Institute of Chemistry, Slovenia

Dr. Alenka Ristić

1.4.1.1.1 *TCM type: composite*

1. Introduction:
New composite water sorbents $CaCl_2$-PHTS for low-temperature sorption heat storage were prepared. The influence of water sorption on the structural properties of the composites of the plugged hexagonal templated silica (PHTS) with different contents of calcium chloride was studied.
2. Preparation of materials and/or supplier:
Novel composites composed of PHTS (plugged hexagonal templated silicate) with hexagonal pore arrangement as the matrix and 4 wt%, 10 wt% and 20 wt% of calcium chloride have been developed by incipient wetness impregnation. PHTS was synthesized by modification of the SBA-15 synthesis using long-chain surfactant triblock copolymer Pluronic P123 to prepare the plugged hexagonal templated silica with ordered hexagonal mesopore arrangement with average pore size lower than 6 nm.
3. Results

The structural, texture and adsorption properties of the matrix and the composites were determined and found out that the water sorption capacity of the composite material depends on the pore size of the matrix, the amount of hygroscopic salt in the pores, the matrix synthesis and the preparation of the composite.

a. Structural properties for porous materials and composites / formula

Table 2. Structural properties of PHTS and the prepared composites.

Sample	S_{BET} (m^2/g)	V_{tot} (cm^3/g)	Average pore size (nm)
PHTS	810	0.705	5.7
4-$CaCl_2$-PHTS	461	0.492	5.6
10-$CaCl_2$-PHTS	322	0.377	5.8
20-$CaCl_2$-PHTS	163	0.189	6.2

S_{BET}, the BET surface area; V_{tot}, total pore volume, mesopore diameters

b. Sorption properties / reaction

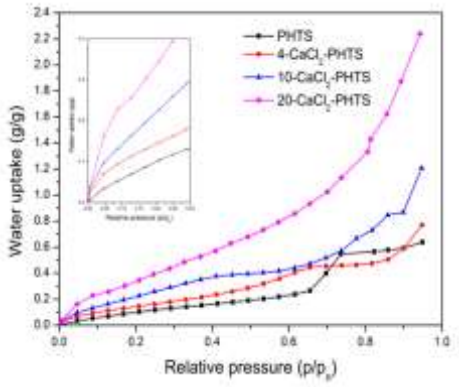

Water uptake curves at 40 °C.

c. Thermochemical properties:

The integral heat of adsorption was calculated for the given boundary conditions: adsorption temperature at 40 °C, desorption temperature at 120 °C and a dew point temperature was set at 10 °C. The integral heat of adsorption Q_{ads} of all composites is listed in Table 2.

Table 3. Water loading lift and the integral heat of adsorption for the composites

Sample	Δw (kg/kg)	Q_{ads} (Wh/kg)	Q_{ads} (kJ/kg)
PHTS	0.073	71	256
4-$CaCl_2$-PHTS	0.100	81	292
10-$CaCl_2$-PHTS	0.142	119	428
20-$CaCl_2$-PHTS	0.239	193	694

d. Picture/image/photograph of the material: Scanning Electron Microscope (SEM) images

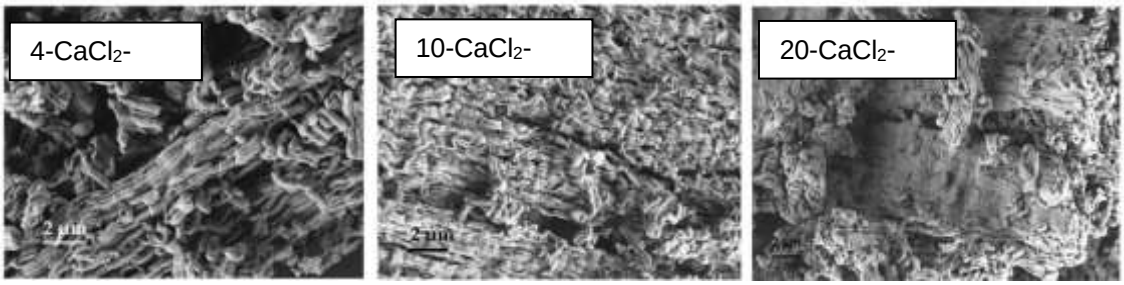

e. Graph: Characteristic curve

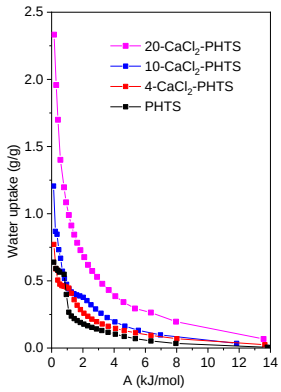

4. Summary:

The increased salt content in the composites impacted the sorption performance of these composites, e.g. higher content of the salt higher energy storage capacity. The storage capacity of these composites can be increased by increasing the desorption temperature and decreasing the adsorption temperature. Water sorption caused structural modifications of the composites, showing the re-dispersion and possible agglomeration of the salt in the pores, which caused some blocking of pores (lower total pore volume and specific surface areas) after hydration and dehydration at 40 ^{o}C. On the other hand, repeated sorption/desorption cycles between 40 and 140^{o}C at 56 mbar caused the improvement of structural properties (increase of specific surface area, total pore volume and pore size) of the 10-$CaCl_2$ and 20-$CaCl_2$ composites, indicating that highly dispersed salt is still present in the pores. During the cyclic test, there was no leaching of the salt from the PHTS matrix, showing the ability of the PHTS matrix to create a stable nano-environment for confinement of calcium chloride.

5. References

RISTIĆ, Alenka, ZABUKOVEC LOGAR, Natasa. New composite water sorbents $CaCl_2$−PHTS for low-temperature sorption heat storage: determination of structural properties. *Nanomaterials*, Jan. 2019, vol. 9, iss. 1, p. 1-16

1.4.1.1.2 *TCM type: sorption material*

1. Introduction:

In this study, a porous zeolite-like aluminophosphate adsorbent with LTA (Linde Type A) topology is inspected as an energy storage and heat transformation material. According to sorption and calorimetric tests, the aluminophosphate outperforms all other zeolite-like and metalorganic porous materials tested so far.

2. Preparation of materials and/or supplier:

APO-LTA was hydrothermally synthesized from a fluoride medium using Kriptofix 222 (K222) as a structure-directing agent. (Krajnc, 2017) The as-synthesized sample was calcined in air at 600 ^{o}C over night.

3. Results

Material shows remarkable cycling stability; after 40 cycles of adsorption/desorption its capacity drops by less than 2%. It adsorbs water in an extremely narrow relative-pressure interval ($0.10 < p/p_0 < 0.15$) and exhibits superior water uptake (0.42 g /g) and energy storage capacity (527 kW h/m^3). Furthermore, its heat pump performance is very high, allowing efficient cooling in demanding conditions with cooling power up to 350 kW h/m^3 even at 30 °C temperature difference between evaporator and environment. Desorption temperature for this material, which is one of crucial parameters in the applications, is lower from desorption temperatures of other tested materials by 10–15 °C. COP and cooling enthalpy for cooling application at boundary conditions: evaporator temperature T_{ev}=5 ^{o}C, cooling temperature T_{con}=30 ^{o}C and desorption temperature T_{des}=65 ^{o}C is determined to be 0.70 and 730 kJ/kg, respectively.

a. Sorption properties / reaction

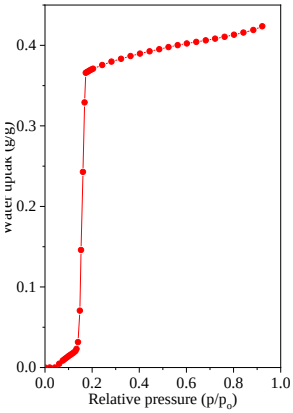

Water uptake curve at 25 °C.

b. Thermochemical properties:

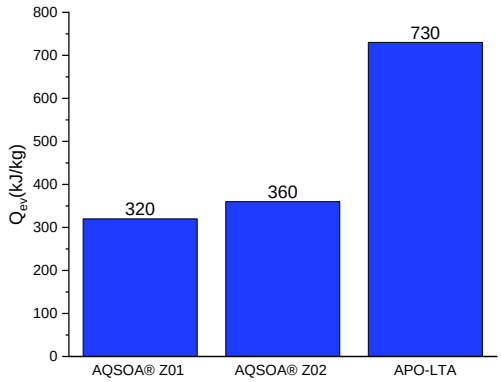

Comparison of the cooling enthalpy Q_{ev} for boundary conditions (T_{ev}=5 °C, T_{con}=30 °C, T_{des}=65 °C)

c. Graph: Characteristic curve

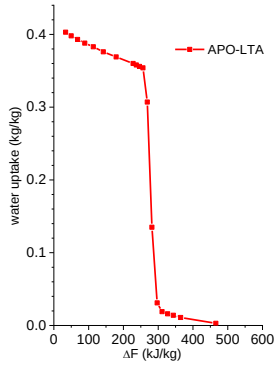

d. Picture/image/photograph of the material:

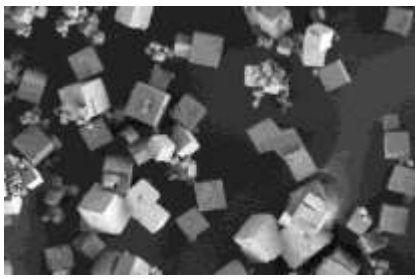

Scanning Electron Microscope image

4. Summary:

New aluminophosphate adsorbent full fills requirements for the ideal performance in the low-temperature (solar energy) heat transformation applications because it performs in the proper relative pressure range with S-shaped water adsorption isotherm. The charging or regeneration temperature is 65 °C. Comparing the cooling enthalpy of AQSOA® Z01 and Z02 adsorbents for air conditioning with regeneration temperature of 65 °C (T_{ev}=5 °C, T_{con}=30 °C) to APO-LTA, the later achieves two times higher cooling enthalpy.

5. References

Krajnc, A., Varlec J., Mazaj, M., Ristić, A., Logar, N.Z., Mali, G., Superior Performance of Microporous Aluminophosphate with LTA topology in solar-energy storage and heat reallocation 2017, Adv. Ener. Mat., 7, 201601815-1.

Alenka Ristić, Andraž Kranjc, Nataša Zabukovec Logar, New water adsorbent for adsorption driven chillers, 8th International Conference on Solar Air Conditioning, September 12-13, 2018, Rapperswil, Switzerland.

1.4.1.2 National Institute of Chemistry, Slovenia and ZAE Bayern, Germany

Dr. Alenka Ristić and Dr. Fabian Fisher

1.4.1.2.1 *TCM type: sorption material*

1. Introduction: We present the use of the commercial granulated binder-free zeolite NaY as the adsorbent for sorption heat storage and the post-synthesis modification of this zeolite in order to decrease the desorption temperature and preserve energy storage density. We have studied the effect of HCl and H_4EDTA treatments, as well as the impact of sequential ion-exchange acid treatment on the material storage performance.

2. Preparation of materials and/or supplier: Binder-free granulated zeolite NaY (parent sample) was supplied from CWK (Bad Köstritz, Germany). Modified samples were prepared using one-step and two-step procedures:

Samples	Treatment	Temperature (°C)	Time (h)
Parent NaY	-	-	-
0025HCl	0.025M HCl	100	1
005HCl	0.05M HCl	100	1
01HCl	0.1M HCl	100	1
005HCl-RT	0.05HCl	RT	120
005EDTA	0.05M H_4EDTA	100	20
MgNaY-0025HCl	1M $Mg(NO_3)_2$;0.025M HCl	85;100	2;1

3. Results

a. Structural properties for porous materials and composites / formula

Less hydrophilic granulated samples can be prepared by nondestructive post-synthesis modifications using mild HCl treatment and chemical treatment with H_4EDTA, leading to a reduction in desorption temperature ranging from 10 to 30 °C. Mild acid treatment caused the generation of defects, which served as a binding sites for water, thus increasing water uptake for 10%. The H_4EDTA treatment introduced mesoporosity and improved the pore accessibility by removal of Al from the framework. On the other hand, a two-step procedure with sequential Mg-exchanged acid treatment can bring about enhanced water sorption capacity and desorption temperature.

b. Sorption properties / reaction

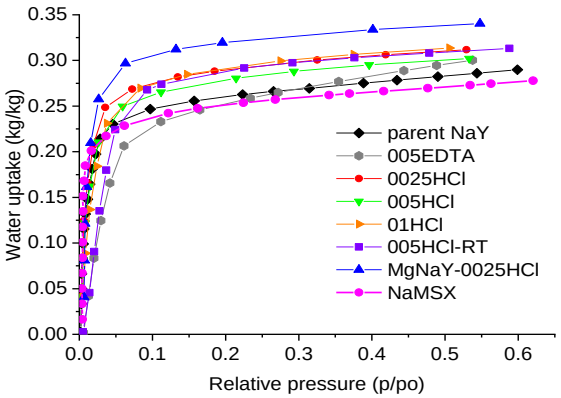

Water uptake at 25 °C of the parent sample NaY, the modified samples and NaMSX.

c. Thermochemical properties:

Water uptake in equilibrium after adsorption (40°C) $X_{S,ad}$ and after desorption (140°C) $X_{S,des}$, water loading spread ΔX_S and the integral heat of adsorption in Wh/kg.

Sample	$X_{S,ads}$ (kg/kg)	$X_{S,des}$ (kg/kg)	ΔX_S (kg/kg)	q_{ads} (Wh/kg)
Parent NaY	0.2898	0.0783	0.2115	**185.0**
0025HCl	0.2931	0.0776	0.2155	**187.9**
005HCl	0.2775	0.0735	0.2040	177.4
01HCl	0.2833	0.0703	0.2130	185.3
005HCl-RT	0.2836	0.0730	0.2106	183.3
005EDTA	0.2573	0.0653	0.1920	166.1
MgNaY-0025HCl	0.3336	0.1331	0.2005	179.4
NaMSX	0.2501	0.1101	0.1400	**127.0**

d. Picture/image/photograph of the material:

SEM image of binder-free zeolite NaY

e. Graph: Characteristic curve

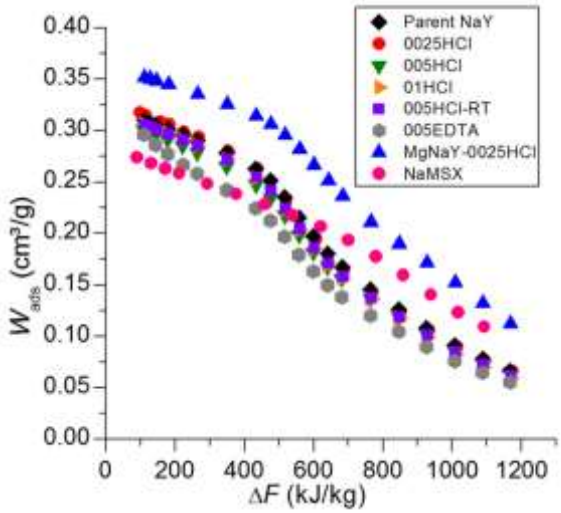

The characteristic curves of the parent NaY, the modified samples and NaMSX

4. Summary:

Commercial granulated binder-free NaY zeolite can be used as the adsorbent in the sorption storage system to recover industrial waste heat at a temperature of 140 °C. The performance of adsorbents in sorption heat storage depended on the type of post-synthesis treatment, for example the H_4DTA treatment improved pore accessibility by removal of Al from the framework, while mild acid treatment caused the generation of defects, which served as the binding sites for water, thus the water uptake was increased. Post-synthesis modifications lead to a reduction in desorption temperature ranging from 10 to 30 °C and to an increase of the evaluated energy storage densities of the parent NaY and the modified samples for up to 40 % above the value of the NaX zeolite at a desorption temperature of 140 °C.

5. References

Ristic, A.; Fischer, F.; Hauer, A.; Logar, N. Z., Improved performance of binder-free zeolite Y for low-temperature sorption heat storage. *Journal of Materials Chemistry A* **2018,** *6* (24), 11521-11530.

1.4.1.3 University of Applied Upper Austria, Research Group ASiC

Dr. Bernhard Zettl and Gayaneh Issayan

1.4.1.3.1 *TCM type: Adsorption*

1. Introduction: the aim of the research

Project OFFSOR-Open Sorption Storage Technology for Building Applications

Project aimed to develope and build a loboratory prototype with automatic cotrol for mass and heat transfer for both, adsroption and desorption cycles. The main goal of thermo-physics were to find measures for adsorption-kinetics that are useful for modelling the heat storage reactions in the relevant set of parameters typical for applications.

2. Preparation of materials and/or supplier

The zeolite granules were purchased in granule form, ready to use and no further sample manipulations accured. Following zeolite molecular sieves were subject to investigation:

- 4A Silkem
- 4A CWK
- 4A BF CWK
- 13X CWK
- 13X BF CWK

3. Results:

a. Structural properties for porous materials and composites / formula

b. Sorption properties / reaction

The utilized zeolites have following properties according to datasheet:

CWK	Type	Pore Size in Å	Granule Size in mm	Adsorption capacity in cm^3/g (min 55% RH, 20°C)	Formula
4A	LTA	4	1,6-2,5	21.5 H_2O	Na_2O . Al_2O_3 . 2.0 SiO_2 · n H_2O
4A BF	LTA	4	2,5-5	24 H_2O	Na_2O . Al_2O_3 . 2.0 SiO_2 · n H_2O
13X	FAU	9	1,2-2	26,5 H_2O	Na_2O . Al_2O_3 . m SiO_2 · n H_2O (m<= 2,35)
13X BF	FAU	9	1,2-2	30 H_2O	Na_2O . Al_2O_3 . m SiO_2 · n H_2O (m<= 2,35)
Silkem					
4A	LTA	-----	2-3,5	-----	Na_20(17-19%), Al_2O_3(28-30%), SiO_2(31-34%), H_2O(18-22%)

c. Thermochemical properties

4A Zeolith: Silikem				
Materialtemperatur	Gasfeuchte	Exposition	Programmierte Temperatur	Quelle für T(Segment|neu)
250°	0 g/kg	240 min	265	STA-sDSC: n18-094
40°	2 g/kg	240 min	46,5	STA-sDSC: n18-094
40°	4 g/kg	240 min	46,5	STA-sDSC: n18-094
40°	6 g/kg	240 min	46,5	STA-sDSC: n18-094
40°	8 g/kg	240 min	46,5	STA-sDSC: n18-094
40°	10 g/kg	240 min	46,5	STA-sDSC: n18-094
160°	10 g/kg	240 min	170	STA-sDSC: n18-094
190°	10 g/kg	240 min	201,5	STA-sDSC: n18-094
220°	10 g/kg	240 min	233	STA-sDSC: n18-094
250°	10 g/kg	240 min	265	STA-sDSC: n18-094
250° (=Start)	0 g/kg	240 min	265	STA-sDSC: n18-094

Figure 1 Temperature and humidity parameters for thermal analysis measurements.

The thermal analysis measurements were executed by DSC/TG. The parameters summed up in Figure 1 describe realistic year-round conditions for material temperature and air humidity. The cycle starts with fully dried material at 250°C. The adsorption in winter can be controlled by increasing the humidity stepwise, which leads to higher material temperature. *Figure 1 Temperature and humidity parameters for thermal analysis measurements.*Those conditions were taken into account for DSC measurements, whereby the exposition time was also specified in Figure 1. The results are depicted in Figure 2.

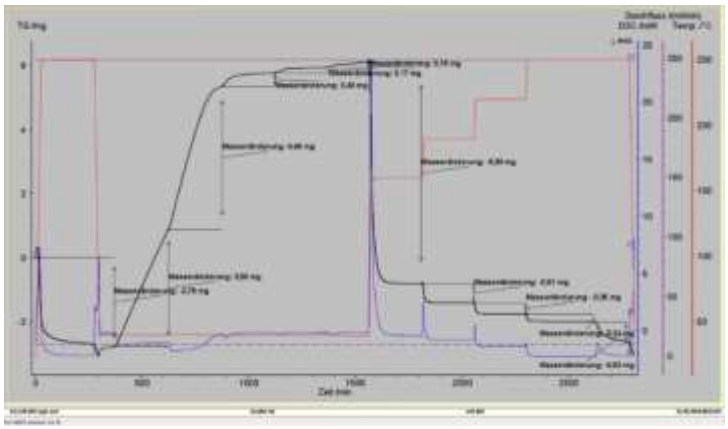

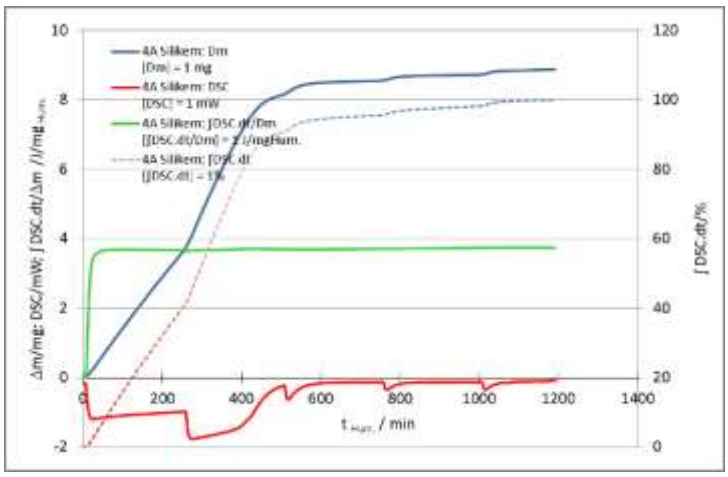

Figure 2: 4A Silkem TG/DSC measurements for one cycle of adsorption and desorption. Measurements by Dr. Wolfgang Hohenauer AIT.

d. Picture/image/photograph of the material

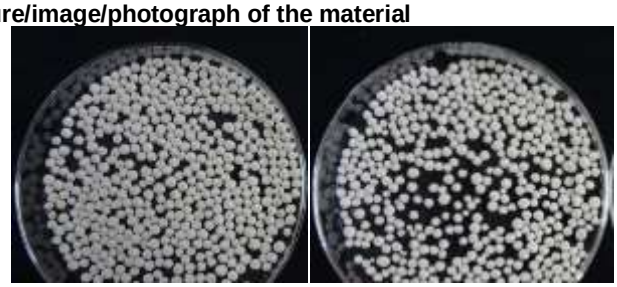

Figure 3 Material 4A BF CWK (left) and 4A Silkem (right).

e. Graph: characteristic curve (adsorbed volume w_{ads} as a function of the adsorption potencial ΔF (kJ/kg))

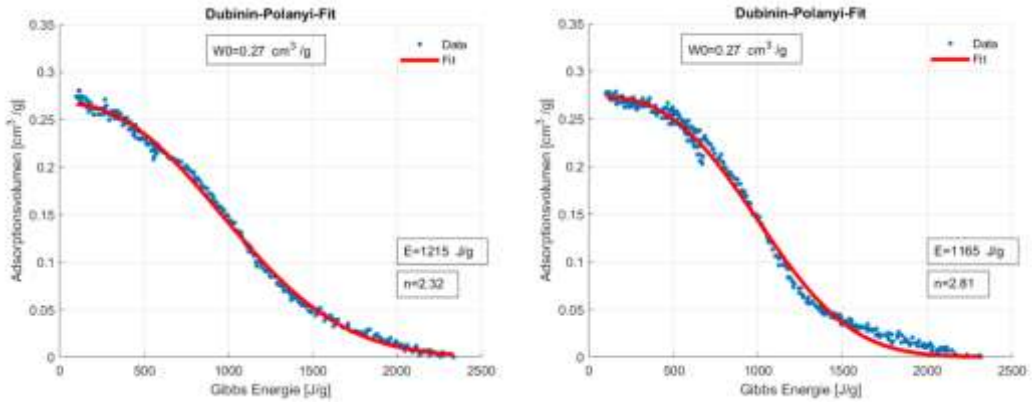

Figure 4 Comparison Characteristic curve of zeolite 4A from different producers: CWK (left) and Silkem (right).

Both zeolites show the same adsorption saturation volume of 0.27 cm^3/g.

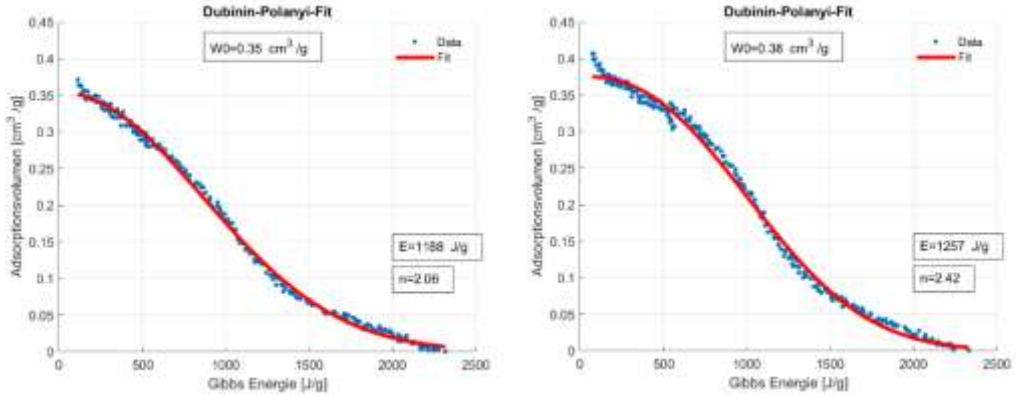

Figure 5 Comparison Characteristic curve of 13X Zeolites (left) and 13 BF (right).

Binder Free zeolites show higher adsorption saturation volume than the ones with binder.

4. Summary

A setup was developed to measure the water vapor adsorption/desorption of zeolites, which had to be purchased in bulk for the designed rotating bed open heat storage (see Figure 6). The selection of appropriate zeolite was supported by the mentioned setup. The measurements results where analysed based on the characteristic curvesThe results showed a constat tendency of higher saturation values for adsorption volume. However the camparison of different materials confirmed the legitimacy of measurement method and the setup. The results show that both 4A zeolite samples purchased from different suppliers yielded the same saturation values and the binder free 13X zeolite indicated a better perfomance regarding the adsorbed volume.

Figure 6 Rotating bed open heat storage prototype developed in Project OFFSOR.

1.4.1.3.2 *TCM type: Chemical reaction-adsorption*

Project New TCM- Development of Highly Efficient Thermochemical Storage Materials

This project aims to investigate and develop stabilization methods of salts and characterize the relevant parameters for process technologies. Disc granulation is chosen to stabilize the salts in combination of porous materials and binders. The granules will be tested on their adsorption capabilities, tensile strength and cycling abilities.

Clinoptilolite IPUS (Ca, K, Na, $Mg)_6(Si,Al)_{36}O\cdot$. $20H_2O$) with high concentration of Ca, less K and rare amounts of Mg and Na. Multiple binder and coating materials in experimental phase. Salt hydrates LiCl anhydrate (Leverton), $CaCl_2$ dihydrate (CIECH Soda Polska) and anhydrate (Carl Roth)

Figure 7: First granulation steps with salts and porous materials.

The project is in process and there are no results available yet.

1.4.1.4 CanmetENERGY Ottawa, Natural Resources Canada and Laboratory for Alternative Energy Conversion (LAEC), School of Mechatronic Systems Engineering, Simon Fraser University

Dr. Lia Kouchachvili, Dr. Redda Djebbar and Prof. Majid Bahrami, Dr. Mina Rouhani

1.4.1.4.1 *TCM types: sorption material, composites and chemical reaction*

Introduction (objectives):
This research aimed at development, characterization, and screening of thermochemical materials to develop high efficient and economically viable thermal energy storage systems.

TCM types:
1- Adsorbent (AQSOA FAM-Z02)
2- Composite sorbents (silica gel+$CaCl_2$; vermiculite+$CaCl_2$)
3- Salt hydrates (Na_2S n.H_2O)

Material preparation/ suppliers

- AQSOA FAM-Z02 (SAPO-34 $Al_{0.56}Si_{0.02}P_{0.42}O_2$) Mitsubishi Plastic Inc

- silica gel+$CaCl_2$; Developed at LAEC

Commercial silica gels (Silicycle Inc., Quebec, Canada) with 4 distinct pore size distributions and 0.2–0.5 mm irregular-shaped grains were wetted with ethanol. Aqueous $CaCl_2$ solution was added to silica. The mixtures were dried for 24 h in a fume hood.The damp material was baked at 200°C until judged dry by successive weight measurements

- Vermiculite+$CaCl_2$; MULTISORB Technologies

Vermiculite (50-75%), $CaCl_2$ (15-50%), High density polyethylene fiber (5 - 15%)

- Na_2S n.H_2O n=0-9; Samples from four different international suppliers

Results – Energy Storage Performance [1,2,3]:
Energy storage density based on dry mass, averaged from the last two cycles:

Sample	Energy storage density (MJ/kg)	Energy storage density (Wh/kg)
AQSOA FAM-Z02	0.963	267.5
silica gel +$CaCl_2$	1.619	449.7
Vermiculite +$CaCl_2$	1.539	427.5
$Na_2S{\cdot}9H_2O$	3.435	954.1
$Na_2S{\cdot}xH_2O$ (commercial-grade)	3.124	867.8

Desorption condition: dry nitrogen with the flow of 20 and 50 ml·min^{-1}, at temperature of **80°C**, and heating rate of 1 K·min^{-1}; **Sorption condition:** temperature of 25°C, and water vapor pressure of 12 mbar (i.e., equivalent to 10°C), and cooling rate (after the desorption and before the sorption) of 5 K min^{-1}.

Summary:
FAM-Z02 showed the highest discharging rate (k_{dch}) of 7×10^{-4} s^{-1}, using $\frac{(\omega-\omega_0)}{(\omega_\infty-\omega_0)} = 1 - \exp(-k_{dch}t)$.
Na_2S n.H_2O provided the highest specific power (SP) and energy storage density (ESD).
Among the rest of sorbent candidates, highest discharge SP (0.431 kWkg^{-1}) was for FAM-Z02 and highest charge SP (0.541 kWkg^{-1}) was for vermiculite+$CaCl_2$.
Silica gel+$CaCl_2$ showed ESD of 1.6 MJkg$^{-1.}$
Due to the low volumetric ESD (low density) of vermiculite+$CaCl_2$, and potential agglomeration of Na_2S n.H_2O samples, the preliminary results seams to point to the silica gel+$CaCl_2$ as a best candidate to explore more.

References:
[1] L. Kouchachvili, R. Djebbar, M. Rouhani, M. Bahrami, (2018) “Characterization of commercial grade sodium sulfide for residential heating applications”, ISEC 2018, Graz, Austria.
[2] M. Rouhani, L. Kouchachvili, R. Djebbar, M. Bahrami, (2019) “Thermochemical energy storage for residential applications”, 5th Experts meeting of IEA SHC T58/ECES A33, Ottawa, Canada.
[3] M. Rouhani, (2019) “Sorption thermal energy storage for sustainable heating and cooling”, PhD Thesis, Simon Fraser University.

1.4.1.5 Swansea University

Dr. Jonathon Elvis

1.4.1.5.1 *TCM type: composite materials*

1. **Introduction (objectives):**
Assessment of energy density, heat evolution (ΔT) and cyclic efficiency of TCM as a function of flow rate (Litres per minute (LPM))

2. **Material preparation/ suppliers**
Vermiculite//$CaCl_2$ synthesised using insipient wetness technique; Vermiculite supplied by Dupre,
$CaCl_2{\cdot}$ XH_2O supplied by Sigma Aldrich

3. Results:
a. Structural properties for porous materials and composites / formula

Vermiculite: $(Mg,Fe^{+2},Fe^{+3})3[(Al,Si)_4O_{10}](OH)2{\cdot}4H_2O$ // $CaCl_2{\cdot}$ XH_2O (X=0,1,2,4,6)

b. Sorption properties / reaction

Typically: $CaCl_2 \cdot 2H_2O \rightarrow CaCl_2 \cdot 6H_2O$

c. Thermochemical properties:

Energy Density: 80 – 250 kWh/m^3

d. Picture/image/photograph of the material

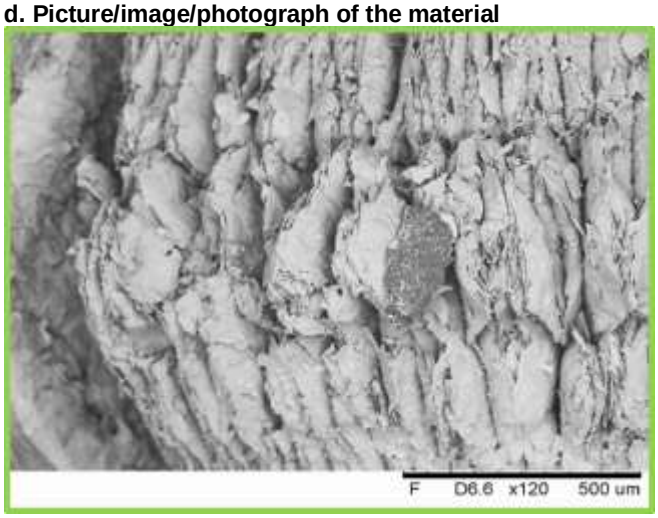

e. Graph: Characteristic curve

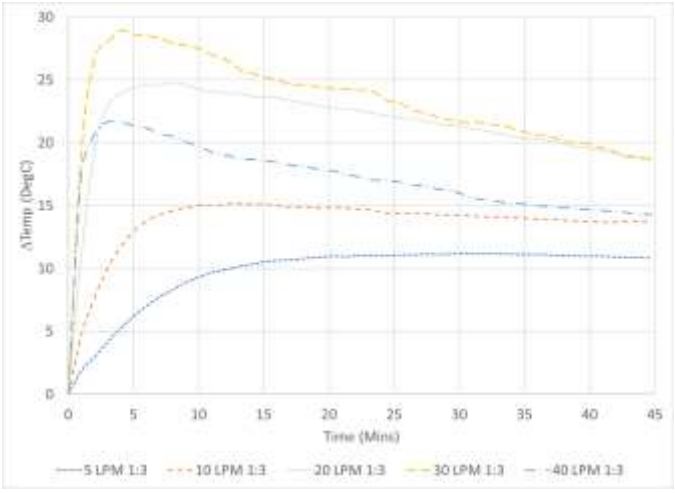

Summary:

Varying the volumetric flow rate has a significant effect upon on both the peak ΔT achieved and the overall energy released during these short term experiments. In these tests, a lower flow rate produces a small temperature rise but allows a more controlled release of energy over the experimental period. As the flow rate is increased up to 30LPM, the ΔT steadily rises as does the overall energy released. Beyond 30LPM, the temperature rise achieved is again reduced, along with the overall energy released.

1.4.2 Chemical reaction

1.4.2.1 Technical University of Denmark (DTU)[1], KTH Royal Institute of Technology- Sweden[2] and IFE- Norway[3], Amminex Emission Technology (AET)- Denmark[4]

Anastasiia Karabanova[1], Dr. Didier Blanchard[1], Dr. Saman Nimali Gunasekara[2], Dr. Viktoria Martin[2], Stefano Deledda[3], Perizat Berdiyeva[3], Benoit Charlas[4]

1.4.2.1.1 *TCM type: chemical reaction*

The reversible chemical reaction system $SrCl_2$-NH_3 is used, specifically for the absorption/ desorption between $SrCl_2 \cdot NH_3$ and $SrCl_2 \cdot 8NH_3$, of which the reaction equation is shown in eq. 1 [1]

$$7\ NH_{3(g)} + SrCl_2 \cdot NH_{3\ (s)} \leftrightarrows SrCl_2 \cdot 8NH_{3\ (s)} + \Delta H\ (41.4\ kJ\ mol^{-1}{}_{NH3}) \qquad eq.\ 1$$

1. Introduction: the aim of the research -Neutrons for Heat Storage (NHS)
The Neutrons for Heat Storage (NHS) project aims to develop a TCS system for low-temperature heat storage (40-80 °C). Here, absorption and desorption between metal halides and NH3 is used. From the project partners, DTU, Denmark, IFE-Norway (collaborating with Amminex Emission Technology (AET) and KTH-Sweden. DTU and IFE are involved in synthesizing and characterizing new mixed metal halides for energy storage using their reaction with ammonia, thermal conductivity improvements of these salts by impregnating these into materials with better thermal conductivity, and performing neutron imaging and numerical modelling (in COMSOL) to characterize the behaviour of the salts in reactors. KTH is involved in designing a bench-scale TCS system and its reactors (with numerical modelling using Aspen plus and COMSOL), for the chemical reaction system $SrCl_2$-NH_3 for simultaneous heat storage and release operation.

2. Preparation of materials and/or supplier
The (pristine) $SrCl_2$ was so far provided by AET, and ENG boards are purchased from SGL carbon GmbH [2]. The $SrCl_2$-ENG composites preparation by impregnation (and in certain cases by mechanical compression), followed by ammoniation of the composite to obtain SrCl2·8NH3-ENG and their characterizations are conducted by DTU. Prior to the composite preparation, the ENG pellet was placed in a vacuum furnace at 120˚C for 12 h to remove any moisture (to measure the right weight of the pellet before impregnation). Then, the pellet was immersed in ethanol (used as a surfactant) for 2 h, to lower the surface tension between the hydrophobic ENG pellet and the aqueous $SrCl_2$ solution. 1. Thereafter, the pellet was taken out of ethanol and immersed in an aqueous $SrCl_2$ solution for 24 h. Afterwards, the pellet was taken out and placed in a ventilated furnace at 90˚C for 12 h to remove the free water, followed by placing in a vacuum furnace at 200˚C for 12 h to remove any water left. Finally, this dried disc was pressed into the desired compaction.

3. Results
Structural properties for porous materials and composites / formula
In the NHS project, initially DTU and IFE synthesized certain new metal halides (e.g. $CaxTiyCuzCl_2$, $CuxCayYzCl_2$, $SrxCayCl_2$, and $NixCayCl_2$) with successful characterization using Differential scanning calorimetry (DSC) and X-ray Diffraction (XRD). However, these alloys failed to produce stable phases. Therefore, the reaction pair $SrCl_2$-NH_3 is then chosen for the project continuation. To improve thermal conductivity of this salt ($SrCl_2$), by DTU, it is then inserted (embedded) into expanded natural graphite (ENG) boards from SGL carbon GmbH [2], to form the composite. With salt impregnation and ammoniation experiments conducted at DTU, the $SrCl_2$-ENG composites were found as can be effectively made to contain 79% w/w% salt in the composite with a bulk density of 615 kg m-3. An example of such prepared composite is shown in Figure 8. The volume expansion after full-ammoniation in this composite was found to be negligible (i.e., the porosity of the ENG board was sufficient to accommodate the $SrCl_2 \cdot 8NH_3$). The thermal properties of this composite are currently under investigation by DTU.

Sorption properties/reaction:
Shown in eq. 1.

Thermochemical properties:

The specific reaction enthalpy for the conversion between $SrCl_2 \cdot NH_3$ and $SrCl_2 \cdot 8NH_3$ is 41.4 kJ molNH3-1 and the entropy is 230 J molNH_3-1 K-1 [3]. The thermal conductivity of both these ammines (pristine) are approximated to be 1.1 W m-1 K-1 [4]. The effective thermal conductivity of the ENG in the bulk $SrCl_2 \cdot 8NH_3$-ENG composite (which includes the porosity of the sample) for in-plane and through-plane directions are considered (using linear regression of available data [2]) as 26 W m-1 K-1 and 10.5 W m-1 K-1 (for the compacted new density of ENG: 172 kg m-3).

Picture/image/photograph of the material

Figure 8. $SrCl_2$ impregnated into ENG.

Graph: characteristic curve

As this system concerns a chemical reaction involving absorption, the characteristic curve is the equilibrium pressure curve. This is compiled into Figure 9 (combined with the phase diagram of NH_3), for absorption-desorption between the monoammine and octaammine of $SrCl_2$. The Van't Hoff's equation, as in eq. 2 [1], [3] expresses the equilibrium pressure of this conversion. In this, p_{eq} is the equilibrium pressure (Pa), p_0 is the reference pressure (1 Pa), ΔH and ΔS are the reaction enthalpy (J/mol) and entropy (J/(mol·K)) respectively, R is the ideal gas constant (8.314 J/(mol·K) and T is the reaction temperature (K).

$$p_{eq} = p_0 \cdot exp\left(-\frac{\Delta H}{RT} + \frac{\Delta S}{R}\right) \qquad \text{eq. 2}$$

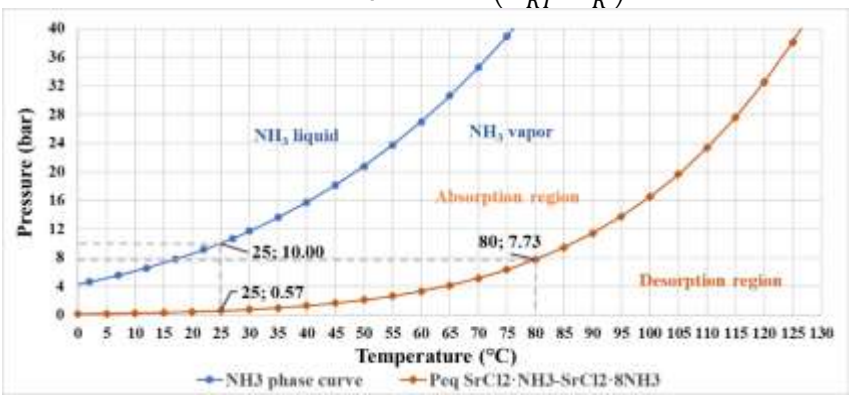

Figure 9. NH_3 phase diagram (based on data from [5]) and $SrCl_2 \cdot NH_3$-$SrCl_2 \cdot 8NH_3$ equilibrium pressure (Peq)-temperature (Teq) plot (based on the Van't Hoff equation, combining data from [1] and [3] into [6])

The reaction kinetic parameters were determined experimentally using a Sieverts-type apparatus, which are compared with literature data as in Table 1. These detailed method and the most updated results are currently being formulated into a scientific article.

Table 1. The comparison of the kinetics parameters from literature and obtained experimentally [8]

Parameter	Absorption		Desorption	
	Literature [7]	Experiment	Literature [7]	Experiment
f(x)	(1-x)2.96	2(1-x)3/2	(1-x)3.02	4(1-x)1/4
k0	0.019	28.1	0.125	1.8*108
Ed	6921	31000	9000	75000
m	1	1	1	0.44

4.Summary

In the NHS project, initially DTU and IFE synthesized certain new metal halides (e.g. $CaxTiyCuzCl_2$, $CuxCayYzCl_2$, $SrxCayCl_2$, and $NixCayCl_2$) with successful characterization using DSC and XRD. However, these alloys failed to produce stable phases. Therefore, the reaction pair $SrCl_2$-NH_3 is then chosen for the project continuation. By DTU, the reaction media is made into composites of $SrCl_2 \cdot 8NH_3$ in ENG (79:21 SrCl2::ENG w/w), for thermal conductivity enhancements. In-addition, DTU has performed kinetic parameters determination of absorption and desorption of the chosen reaction pair ($SrCl_2 \cdot NH_3$ and $SrCl_2 \cdot 8NH_3$) using a Sieverts-type apparatus. KTH is in the process of designing and constructing a bench-scale TCS system for the same reaction pair with two identical reactors (0.5 kWh storage capacity each). The reactor is of a cylindrical packed-bed type, combined with a heat exchange unit. Some of these results of these various study aspects of the NHS project were already presented and published at several conferences with some more planned to be presented in certain upcoming conferences and into journal manuscripts.

Presentations and publications

1) Anastasiia Karabanova, Perizat Berdiyeva, Didier Blanchard, Rune E. Johnsen, Stefano Deledda Comparison between Numerical Simulation and Neutron Radiography of Ammonia Sorption in SrCl2 for Application in Thermochemical Storage System for Waste Heat Recovery, Eurotherm Seminar n-112: 15-17 May 2019, Spain.

2) P. Berdiyeva, A. Karabanova, D. Blanchard, R. E. Johnsen, B.C. Hauback S. Deledda, Neutron Imaging study of Strontium Chloride Ammine system for Heat Storage, Workshop on neutron imaging and scattering on engineering materials (Dec. 6.-7, 2018 in Copenhagen)

3) Saman Nimali Gunasekara, Michail Laios, Anastasiia Karabanova, Viktoria Martin and Didier Blanchard, 2019. Design of a bench-scale ammonia-SrCl2 thermochemical storage system using numerical modelling. Eurotherm Seminar n-112 (http://eurotherm.udl.cat/), Lleida, Spain. 15-17 May 2019.

4) Saman N. Gunasekara, Stefano Soprani, Anastasiia Karabanova, Viktoria Martin and Didier Blanchard, 2019. Numerical Design of a Reactor-Heat Exchanger Combined Unit for Ammonia-SrCl2 Thermochemical Storage System. ISES SWC-2019 (https://www.swc2019.org/home.html), 4-7 Santiago, Chile. (Will deliver an oral presentation)

References

[1] S. Soprani, "MODELING – TES system based on SrCl2 - NH3," Technical University of Denmark (DTU), Lyngby, 2017.

[2] SGL Carbon GmbH, "SIGRATHERM L and LN - Graphite lightweight board for tehrmal management.," SGL Carbon GmbH, 2019. [Online]. Available: https://www.sglcarbon.com/en/markets-solutions/material/sigratherm-graphite-lightweight-board/. [Accessed 29 August 2019].

[3] S. Lysgaard, A. L. Ammitzbøll, R. E. Johnsen, P. Norby, U. J. Quaade and T. Vegge, "Resolving the stability and structure of strontium chloride amines from equilibrium pressures, XRD and DFT," International Journal of Hydrogen Energy, vol. 37, pp. 18927-18936, 2012.

[4] L. Jiang, L. W. Wang, Z. Q. Jin, R. Z. Wang and Y. J. Dai, "Effective thermal conductivity and permeability of compact compound ammoniated salts in the adsorption/desorption process," International Journal of Thermal Sciences, vol. 71 , pp. 103-110, 2013.

[5] e. John R. Rumble, "Fluid Properties - Vapor Pressure of Fluids at Low Temperatures," in CRC Handbook of Chemistry and Physics, 99 ed., vol. 99th Print Edition (Internet Version 2018), Boca Raton, FL, CRC Press/Taylor & Francis.

[6] S. N. Gunasekara, M. Laios, A. Karabanova, V. Martin and D. Blanchard, "Design of a bench-scale ammonia-SrCl2 thermochemical storage system using numerical modelling," in Eurotherm Seminar n-112- Advances in Thermal Energy Storage, Lleida, 2019.

[7] H.-J. Huang, G.-B. Wu, J. Yang, Y.-C. Dai, W.-K. Yuan and H.-B. Lu, "Modeling of gas–solid chemisorption in chemical heat pumps," Separation and Purification Technology , vol. 34, p. 191–200, 2004.

[8] A. Karabanova, P. Berdiyeva, S. Soprani, R. E. Johnsen, S. Deledda and D. Blanchard, "Comparison between Numerical Simulation and Neutron Radiography of Ammonia Ab- and Desorption in SrCl2 for Application in Thermochemical Storage System for Waste Heat Recovery," in Eurotherm Seminar nr. 112-Advances in Thermal Energy Storage, Lleida, 2019.

[9] A. Erhard, K. Spindler and E. Hahne, "Test and simulation of a solar powered solid sorption cooling machine," International Journal of Refrigeration, vol. 21, no. 2, pp. 133-141, 1998.

1.4.2.2 Materials Science & Eng. Department Northwestern University, Evanston, USA Institute of Catalysis and Petrochemistry, Sperior Council for Scientific Research, Madrid, Spain

Dr. Emauela Mastronando

1.4.2.2.1 *TCM type: chemical reaction*

1. Introduction:
In this study Fe-doped CaMnO3 perovskites have been investigated for high temperature thermochemical heat storage. The working principle of a TCS system based on perovskite consists of the following reaction: $ABO_3 \pm \delta 0$(s) ⇌ $ABO_3 \pm \delta 0-\delta$ (s) $+\delta 2O_2$ (g) (2)
Where, δ0 is the initial oxygen non stoichiometry and thus (3±δ0) stands for the initial oxygen content in the material. The reduction, being endothermic, comprises the heat storage step, whereas the exothermic oxidation releases heat when it is required. The heat that can be stored (chemical heat) is directly proportional to the reduction/re-oxidation enthalpy and extent (δ).
$CaMnO_3$ oxide can be considered a promising candidate since it is able to release oxygen in a wide temperature range (800-1000 °C) at different oxygen partial pressures (pO2) suitable for Concentrated Solar Power (CSP) plants. However, it undergoes decomposition at pO2<0.008 atm and at temperature ≥ 1100 °C. In order to overcome this limitation and to extend the operating temperature range, in this study B-site doping with Fe ($CaFe_xMn_{1-x}O_3$-δ0) was used as approach for preventing its decomposition.
The thermodynamic parameters were determined through the van't Hoff approach [1] applied to thermogravimetric profiles obtained at different oxygen partial pressures.

2. Preparation of materials
Fe-doped $CaMnO_3$ samples ($CaFe_xMn_{1-x}O_3$), with a dopant amount (x) of 0.1 were prepared according to a modified Pechini method as reported in literature [2].

Composition	Code	Dopant
CaMnO3-δ0	CM	0
CaMn0.9Fe0.1O3-δ0	CMF91	0.1

3. Results:
a. Structural properties
The X-Ray Diffraction (XRD) patterns (see Figure 1) perfectly match that of Pnma orthorhombic $CaMnO_3$ (PDF 04-007-8030). No other phases were detected. Hence, 10 at% Fe is incorporated into the $CaMnO_3$ structure without the formation of any secondary phase. A shift toward lower 2-theta angles reflects a slight increase in the lattice parameters (and the unit cell volume), in response to the Fe doping. A slight broadening of the peaks similarly reflects the incorporation of the dopant into the structure.

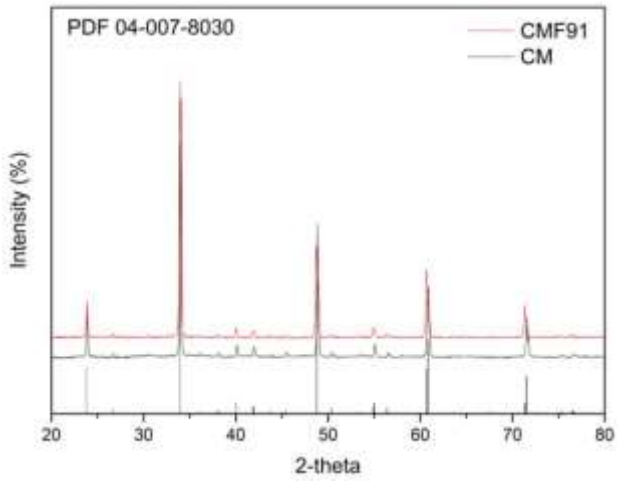

Figure 1. XRD pattern of un-doped and Fe-doped $CaMnO_3$.

b. Thermochemical properties

Thermogravimetric (TG) analysis in the temperature range 200-1200 °C under a pO2=0.008 atm have been carried on the as prepared samples. From CM profile it can be observed that the sample is not able to fully re-oxide. XRD analysis of the sample after TGA detected the presence of residual spinel structure ($CaMn_2O_4$) which most likely prevented the complete re-oxidation of the sample. In case of Fe-doped $CaMnO_3$, oxygen begins to be released at lower temperature with respect to CM. Moreover, the reduction process is fully reversible for CMF91 sample.

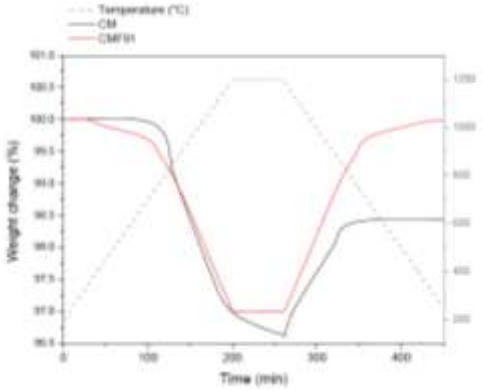

Figure 2. TG profiles of CM and CMF91 under a pO2=0.008 atm.

c. Picture/image/photograph of the material

Cilindric porous pellets used for TG analysis for the extraction of the thermodynamic data.

Figure 3. Cilindric porous pellets used for TG analysis.

d. Graph: characteristic curve (QM (kJ/kgABO3) Vs. Temperature)

The heat storage capacity of the two materials as a function of temperature for pO2=0.008 atm is shown in Figure 4. This analysis reveals that CMF91 has a higher heat storage capacity (344.3 ± 0.6 kJ/kgABO3 or 639.0 ± 1.1 MJ/m3) than CM (272.5 ± 1.1 kJ/kgABO3 or 315.3 ± 1.3 MJ/m3). In addition, at equal pO2, CMF91 is also able to

store heat up to higher temperature (1200 °C), thus widening the operating temperature range. A small quantity of heat can also be stored between 400-800 °C.

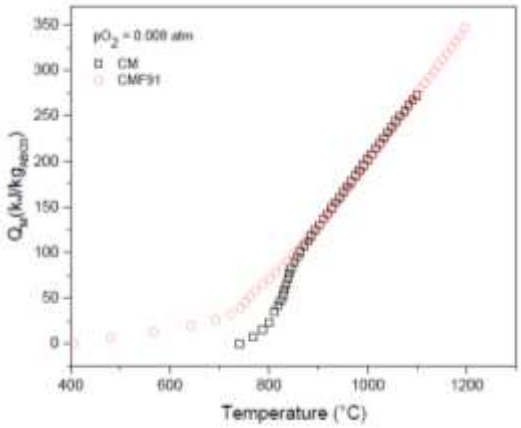

Figure 4. Heat storage capacity of the two materials as a function of temperature for pO2=0.008 atm.

4. Summary

In this study, CaMn0.9Fe0.1O3 oxide, formed of earth-abundant, inexpensive, non-toxic elements, has been investigated as a possible heat storage material for concentrated solar power plants. It has been demonstrated that the presence of Fe allows the CaMnO3 to operate at higher temperature (1200 °C) than the un-doped material, thus increasing the reversible reduction oxidation extent. Indeed, Fe-doping prevented the irreversible decomposition of CaMnO3 above 1100 °C for pO2<0.01. The heat storage capacity (QM) has been estimated to be ~344 kJ/kgABO3. Moreover, in case of the Fe-doped CaMnO3 the oxygen release onset temperature is lowered below 400 °C and the reduction can be carried out up to 1200 °C, thus widening the operating temperature range.

5. References

[1] Y. Hao, C. K. Yang, and S. M. Haile, Chem. Mater. 26, pp. 6073–6082 (2014).
[2] D. Sastre, A.J. Carrillo, D.P. Serrano, P. Pizarro, J.M. Coronado, Top. Catal. 60, pp. 1108–1118 (2017).

Acknowledgments

This project has received funding from the European Union's Horizon 2020 research and innovation programme under the Marie Sklodowska-Curie grant agreement N° 74616. Support of the US Department of Energy, Office of Energy Efficiency and Renewable Energy, Award DE-EE0008089.0000, is also acknowledged.

1.4.2.3 University of Messina – Engineering Department

Prof. Candida Milone

1.4.2.3.1 *TCM type: chemical reaction*

1. Introduction:

Newly developed hybrid materials made of magnesium hydroxide deposited onto expanded graphite (EG), pristine and functionalized carbon nanotubes (*p*-CNT, *f*-CNT respectively) were proposed as heat storage medium for $MgO/H_2O/Mg(OH)_2$ chemical heat pumps.

2. Preparation of materials and/or supplier:

Samples were synthesized by deposition-precipitation (DP) method.

3. Results

a. Structural properties for porous materials and composites / formula

$Mg(OH)_2$ supported on expanded graphite/pristine and functionalized CNT

b. Sorption properties / reaction

$Mg(OH)_2$ (s) ↔ MgO (s) + H_2O (v) $\Delta H_0 = \pm$ 1389 kJ/$kg_{Mg(OH)2}$

c. Thermochemical properties:

The performances of the synthesized materials were evaluated by thermogravimetric analysis, which simulates the chemical heat pump cycle.

d. Picture/image/photograph of the material: Scanning Electron Microscope (SEM) images

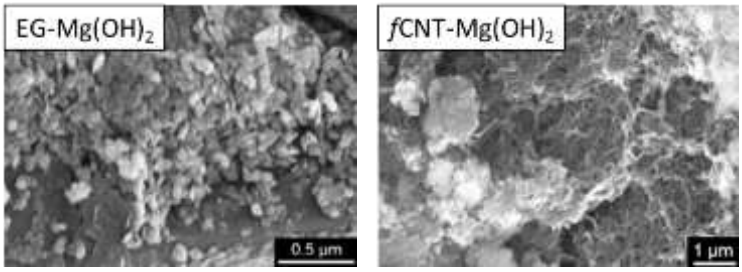

e. Graph:

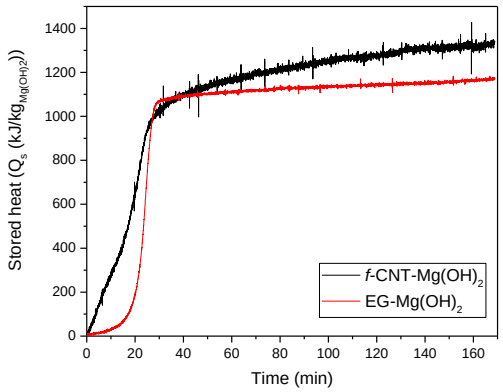

4. Summary :

As main results it is found that :i) at given $Mg(OH)_2$ load DP method allows to enhances the thermochemical performance of hybrid materials; ii) heat storage/output capacities of EG-$Mg(OH)_2$ ($Mg(OH)_2$ = 50 wt%) approaches 1200 kJ/$kg_{Mg(OH)2}$); iii) *f*-CNT-$Mg(OH)_2$ (30 wt% $Mg(OH)_2$) reaches the highest heat storage/output capacities (≈1300 kJ/$kg_{Mg(OH)2}$).

5. References

• E. Mastronardo, L. Bonaccorsi, Y. Kato, E. Piperopoulos, M. Lanza, C. Milone. Strategies for the enhancement of heat storage materials performances for MgO/H_2O/$Mg(OH)_2$ thermochemical storage system. Applied Thermal Engineering 120 (2017) 626-634. DOI: 10.1016/j.applthermaleng.2017.04.004

• E. Mastronardo, Y. Kato, L. Bonaccorsi, E. Piperopoulos, C. Milone. Thermochemical storage of middle temperature wasted heat by functionalized C/Mg(OH)2 hybrid materials. Energies 10 (2017) 70. DOI: 10.3390/en10010070

• E. Mastronardo, Y. Kato, L. Bonaccorsi, E. Piperopoulos, C. Milone. "Thermochemical Storage of Middle Temperature Wasted Heat by Functionalized C/Mg(OH)2 Hybrid Materials" Energies 10, (2017),70-86 (16 pp)

1.4.2.3.2 *TCM type: chemical reaction*

1. Introduction:

Pure $Mg(OH)_2$ (MH) shows a poor durability to several dehydration/hydration reactions, decreasing its reacted fraction to ~50% after only three cycles. The performance implementation of this storage medium is still object of study. Here, it has been investigated how the heat storage capacity of $Mg(OH)_2$ is influenced by the dispersing agent addition during the synthesis.

2. Preparation of materials and/or supplier:

Samples were synthesized by deposition-precipitation (DP) method in the presence of cationic surfactant, cetyl trimethyl ammonium bromide (CTAB) that is used as a dispersing agent for inhibiting the natural tendency of $Mg(OH)_2$ to aggregate.

3. Results

a. Structural properties for porous materials and composites / formula

$Mg(OH)_2$ powder

b. Sorption properties / reaction

$Mg(OH)_2$ (s) ↔ MgO (s) + H_2O (v) $\Delta H_0 = \pm$ 1389 $kJ/kg_{Mg(OH)2}$

c. Thermochemical properties:

The performances of the synthesized materials were evaluated by thermogravimetric analysis, which simulates the chemical heat pump cycle.

d. Picture/image/photograph of the material: Scanning Electron Microscope (SEM) images

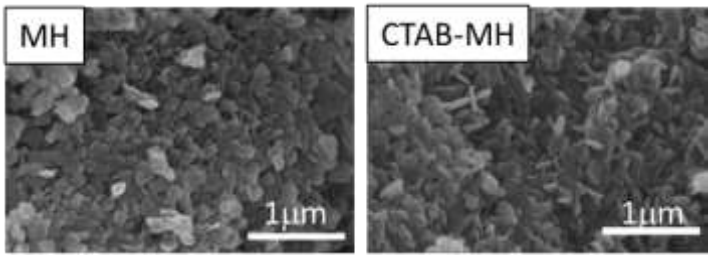

e. Graph:

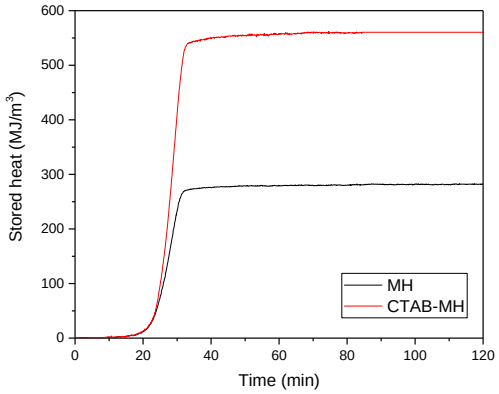

4. Summary:

The results obtained show that CTAB addition promotes the formation of well separated $Mg(OH)_2$ particles. Moreover, CTAB-MH sample exhibits the highest volumetric stored/released heat capacity, ~ 560 MJ/m^3, almost 2 times higher than that measured over $Mg(OH)_2$ prepared in absence of CTAB. Cyclic experiments evidence an excellent stability of the sample up to 13 dehydration/hydration reactions. That means, for technological application, smaller volume at equal stored/released heat.

5. References

- Emanuela Mastronardo, Lucio Bonaccorsi, Yukitaka Kato, Elpida Piperopoulos, Maurizio Lanza, Candida Milone. “Strategies for the enhancement of heat storage materials performances for $MgO/H_2O/Mg(OH)_2$ thermochemical storage system” Applied Thermal Engineering 120, (2017), 626-634.
- Elpida Piperopoulos, Emanuela Mastronardo, Marianna Fazio, Maurizio Lanza, Signorino Galvagno, Candida Milone. “Enhancing the volumetric heat storage capacity of Mg(OH)2 induced by the addition of a cationic surfactant during its synthesis” Applied Energy 215 (2018) 512-522.

1.4.2.3.3 *TCM type: chemical reaction*

1. Introduction:

Metal (Ca^{2+}, Ni^{2+}, and Co^{2+}) doped $Mg(OH)_2$ (MH) was investigated to study the doping effect on the thermochemical (TCM) material's behaviour. Metal ions (Me) were inserted in $Mg(OH)_2$ matrix and the subsequent materials were structurally, morphologically and thermochemically characterized.

2. Preparation of materials and/or supplier:

The synthesis was conducted by precipitation method, using 50 mL of a solution containing Mg^{2+} and the metal ion (Ca^{2+} or Ni^{2+} or Co^{2+}) in a nominal molar ratio Me/Mg^{2+} of 0.2. This was gradually added to 150 mL of NH_4OH solution, under magnetic stirring. The resulting solution was aged at ambient temperature for 24 h, then it was vacuum filtered; the collected solid was washed with deionized water and dried in a vacuum oven at 50 °C overnight.

3. Results

a. Structural properties for porous materials and composites / formula

Doped $Mg(OH)_2$ powder

b. Sorption properties / reaction

$Mg(OH)_2$ (s) ↔ MgO (s) + H_2O (v) $\Delta H_0 = \pm$ 1389 kJ/$kg_{Mg(OH)2}$

c. Thermochemical properties:

The performances of the synthesized materials were evaluated by thermogravimetric analysis, which simulates the chemical heat pump cycle.

d. Picture/image/photograph of the material: Scanning Electron Microscope (SEM) images

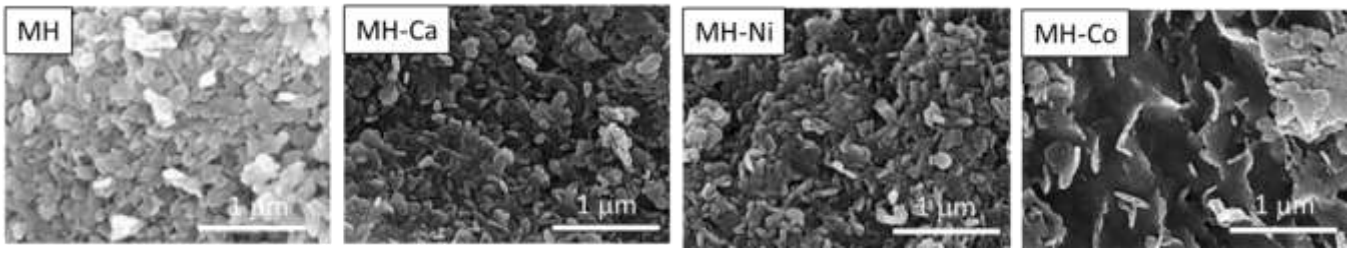

e. Graph:

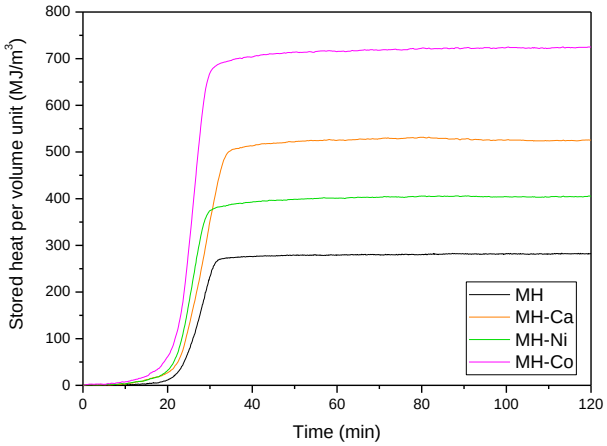

4. Summary:

The obtained results show that metal doping strictly influences morphological and structural properties. The apparent density increase effects the volumetric stored/released heat capacity. The highest value is reported for MH-Co sample (725 MJ/m^3), and it is almost three times higher than MH's value.

5. References

- Elpida Piperopoulos, Marianna Fazio, Emanuela Mastonardo “Synthesis of Me Doped $Mg(OH)_2$ Materials for Thermochemical Heat Storage”, Nanomaterials, 8 (2018) 573-590

1.4.2.4 CIC energiGUNE Spain,

Dr. Stefania Doppiu

1.4.2.4.1 *TCM type: chemical reaction*

1. **Introduction**:
The aim of the investigations is the development of thermal energy storage materials for high temperature applications (above 250 ˚C). This includes the synthesis, the modification, the structural characterization and the TES performance optimization. The materials investigated are based on solid-solid chemical reactions (eutectoids and peritectoids) and solid-liquid chemical reactions (peritectics) in salt-based and metals-based binary mixtures.

2. **Preparation of the materials**:
Solid-solid reactions: The materials were studied as received (testing the performances without modification) and after modification (synthesis of nanostructured materials bay ball milling techniques) to increase the reactivity in the solid state and to Investigate the relationship between microstructure and reactivity. **Solid-liquid reactions:** The materials were studied as received and after addition of nanoparticles and infiltration in porous matrixes (preparation of hybrid materials) to increase the reactivity.

3. **Results**: **Solid-solid reactions**:
In the system Li_2SO_4/Na_2SO_4 two compositions (an eutectoid reaction and a solid-solid phase transition) have been identified with very promising TES performances (enthalpies between 185 - 190 kJ/kg and 160 kJ/kg respectively). The DSC (three cycles) relevant to the two compositions are shown in Figure 1a. **Solid-liquid reactions**: The peritectic composition in the system LiOH/LiBr presents an enthalpy of reaction + melting of 284 kJ/kg. If the sensible contribution is taken into account (ΔT = 60 ˚C) the total energy is 382 kJ/kg (Enthalpy of reaction and reaction + melting relevant to each point studied in the phase diagram are shown in Figure 1 b).

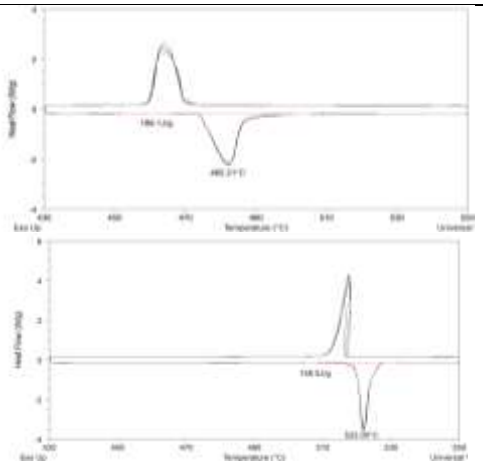

(a)

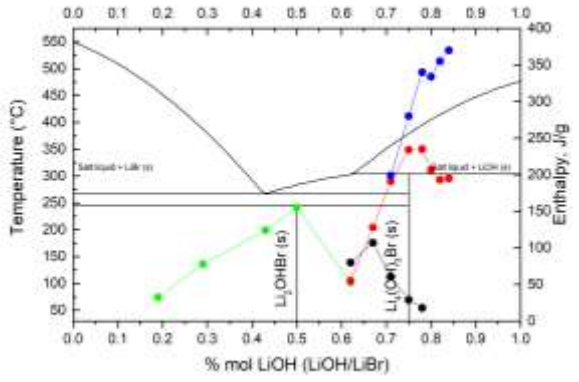

(b)

Figure 1: a) solid-solid reaction and b) solid-liquid reactions

4. Summary:
The investigation allowed to identify several promising solid-solid and solid liquid chemical reactions and transitions for TES at high temperature. Th work is still going on in order to maximize the reactivity of both systems and to clarify some discrepancies obtained from the theoretical studies.

5. References:

1) Doppiu, S., Dauvergne, J. L., & Palomo del Barrio, E. (2019). “Solid-State Reactions for the Storage of Thermal Energy”. Nanomaterials, 9(2), 226. 2) Mahroug, I; Doppiu, S.; Palomo Del Barrio, E.; “Peritectic compounds for thermal energy storage: Experimental investigation and optimization”, XI Congreso Nacional y II Internacional de Ingeniería Termodinámica, Albacete (2019)

1.4.2.5 Institute of Applied Synthetic Chemistry (TU Wien)

Dr. Peter Weinberger

1.4.2.5.1 *TCM type: Chemical reaction*

1. Introdution

The de-respectively rehydration behaviour of CaC_2O4 x H_2O was studied via thermal analysis and powder X-ray diffraction (PXRD). Furthermore, Cycle stability of the material was tested by a long-term stress experiment involving 100 charging and discharging cycles.

2. Preparation of materials and/or supplier

- Calcium oxalate monohydrate (CAS 5794-28-5) was obtained from Sigma-Aldrich and used as supplied.

3. Results

Material: Calcium oxalate monohydrate

Chemical formula: CaC_2O_4 x H_2O

Reactive gas: H_2O

The hydration behavior of $CaC_2O_4 \cdot H_2O$ is quite unusual compared to other salt hydrates that are considered as TCES material, since, depending on water vapour concentration the hydration reaction can occur well above 100 °C. An increased water vapour concentration shifts the phase stability boundary towards higher temperatures, thus extending the stability regime of the hydrate phase. In absolute values, the $peak_{max}$ temperature for the rehydration reaction is shifted from 157.1 °C for a vapour concentration of 0.4 g H_2O h^{-1} ($p(H_2O)$=0.084 bar) to 199.8 °C for 5 g H_2O h^{-1} ($p(H_2O)$=0.53 bar)(Fig. 1a and b).

Cycle stability of the material was tested by a long-term stress experiment involving 100 charging and discharging cycles where no signs of material fatigue or reactivity loss were found (Fig. 2a and b).

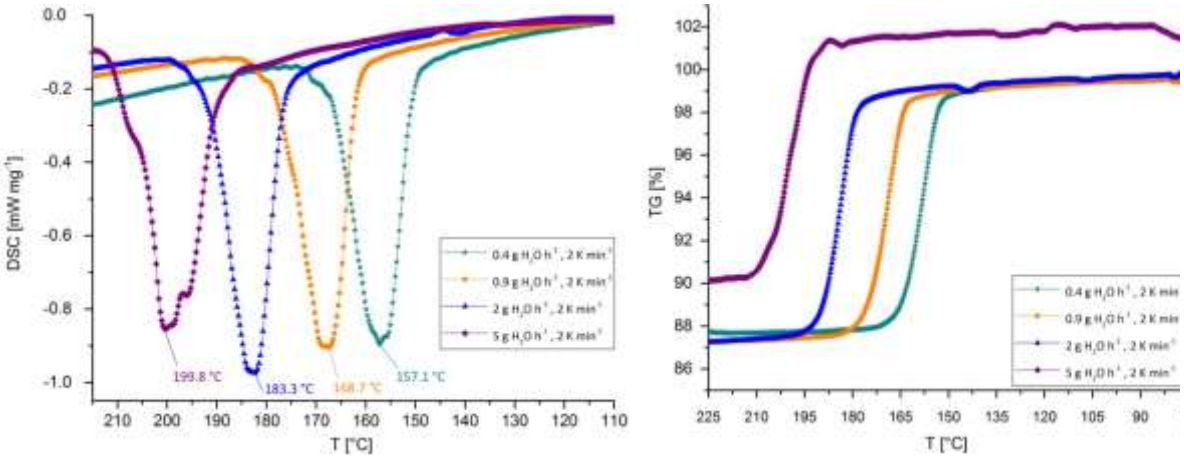

Fig. 10a: Heat-flow of the rehydration reaction with respect to the water vapour concentration; b: Mass-change during the rehydration reaction with respect to the water vapour concentration. For all 4 curves full conversion was achieved. The shift of the 5 g H_2O h^{-1} curve about 2 % is caused by condensation issues.

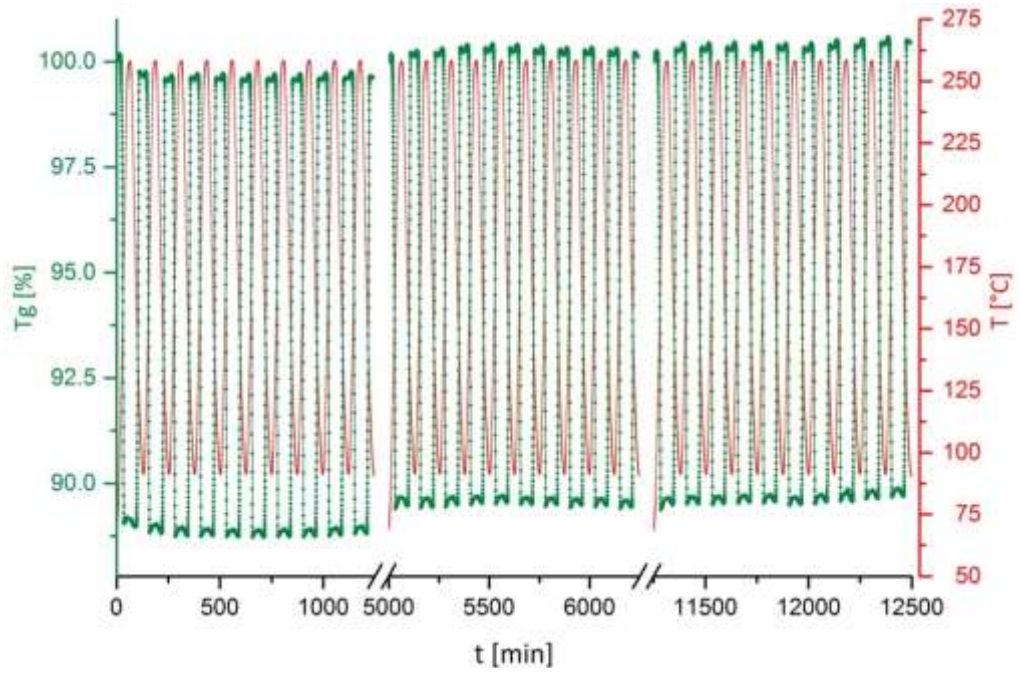

Fig. 2a TG-curve of cycles 1-10, 51-60 and 91-100 of the $CaC_2O_4 \cdot H_2O$ dehydration / rehydration reaction with 0.5g H_2O h^{-1}, 5 K min^{-1}.

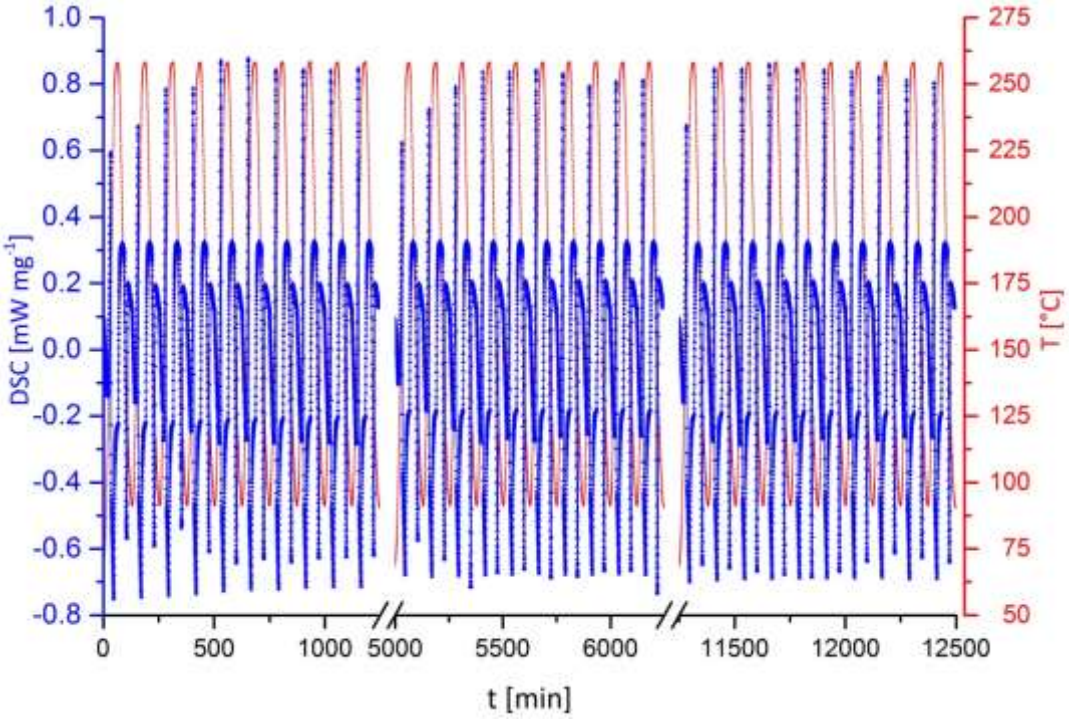

Fig. 2b DSC-curve of cycles 1-10, 51-60 and 91-100 of the $CaC_2O_4 \cdot H_2O$ dehydration / rehydration reaction with 0.5g H_2O h^{-1}, 5 K min^{-1}.

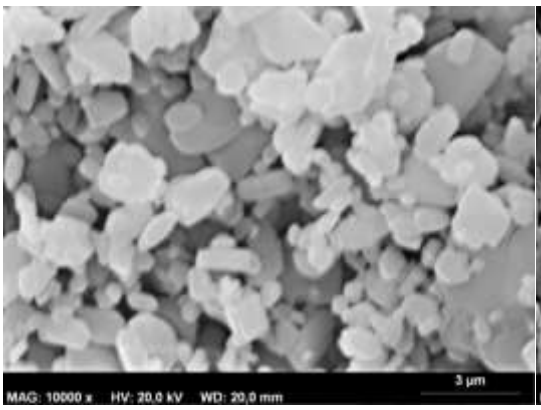

Fig. 3a: $CaC_2O_4 \cdot H_2O$, starting material

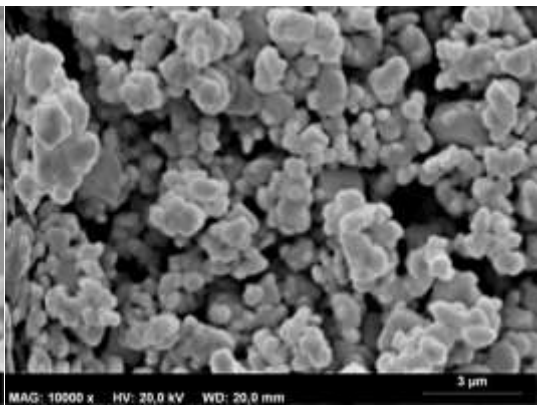

Fig. 3b: Figure 3b: CaC_2O_4, anhydrate phase before 1st cycle

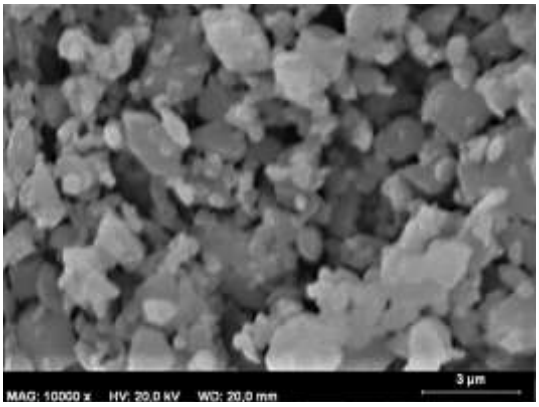

Fig. 3c: $CaC_2O_4 \cdot H_2O$ after 10 cycles

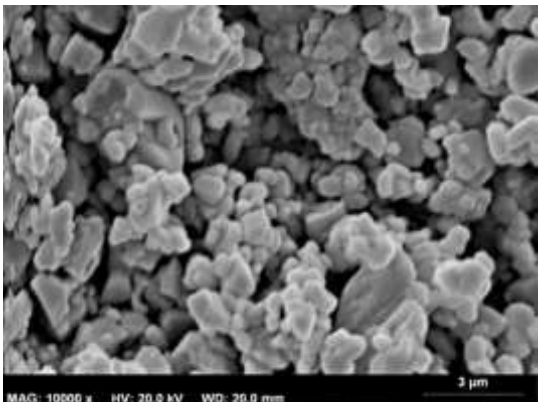

Fig. 3d: $CaC_2O_4 \cdot H_2O$ after 100 cycles

4. Summary

The properties rendering calcium oxalate an attractive material for technical TCES application, in addition to cycle stability and the rapid conversion evidenced in the P-XRD, the most interesting property of this system is its broad operational range. Most salt hydrates considered for TCES purposes form their hydrate at temperatures below 100 °C. $CaC_2O_4 \cdot H_2O$ is unusual in this regard, since, depending on water vapour concentration the release of the stored energy can occur well above 100 °C. This would allow for release of the stored heat at temperatures only slightly below the charging temperature. For industrial purposes it is preferable that the temperature difference between charging and discharging reactions be small, leading to a high exergy. An increased water vapour concentration shifts the phase stability boundary towards higher temperatures, thus extending the stability regime of the hydrate phase. These shifts of the peak temperature related to the vapour concentration allow for a potential application as a chemical heat pump, thus having a broad operational possibility at high temperatures. Our results state an operational range between room-temperature and 200 °C. This region may be further extended by higher water vapour concentrations.

5. References

Knoll et al., "Probing cycle stability and reversibility in thermochemical energy storage–$CaC_2O_4 \cdot H_2O$ as perfect match?." Applied energy 187 (2017): 1-9.

1.4.2.5.2 *TCM type: chemical reaction*

1. Introdution

Calcium doping of magnesium oxide results in significantly increased water dissociation rates, thus enhancing both hydration rate and reaction completeness of hydration compared to pure MgO. A series of mixed magnesium-calcium oxides ($Mg_xCa_{1-x}O$) with varying Ca contents between 0% and 40% was synthisized and the reaction itself was followed via in situ powder X-ray diffraction (P-XRD).

2. Preparation of materials and/or supplier

Mixtures of the appropriate amounts of $MgCl_2 \cdot 6H_2O$ and $CaCl_2 \cdot 6H_2O$ to produce 0.2 mol of the mixed oxide, were dissolved in 75 ml degassed H_2O. Freshly prepared 20 % NaOH solution in degassed H_2O (0.4 mol, 50 ml) were added, resulting in immediate precipitation of a voluminous white precipitate. The $Mg_xCa_{1-x}(OH)_2$ precipitated was centrifuged and washed three times with 100 ml degassed H_2O until chloride free (verified by silver-nitrate test). The hydroxides were calcined in an electric furnace under static atmosphere for 4 hours at 375 °C, yielding the oxides of the composition $Mg_xCa_{1-x}O$, where x= 1-0.5 in almost quantitative yields.

3. Results

Material: Calcium doped magnesium oxide - (Mg,Ca)O)

Chemical formula: (Mg,Ca)O

Reactive gas: H_2O

All experimentally investigated Ca^{2+}-doped oxides show a significantly higher rehydration rate than a commercial MgO sample which was used as reference sample. The fastest reaction rate was found for $Mg_{0.9}Ca_{0.1}O$ for which, after 80 min, the oxide was completely converted to the mixed hydroxide. For larger Ca^{2+} amounts, the final conversion decreased slightly to roughly 80% hydroxide phase.

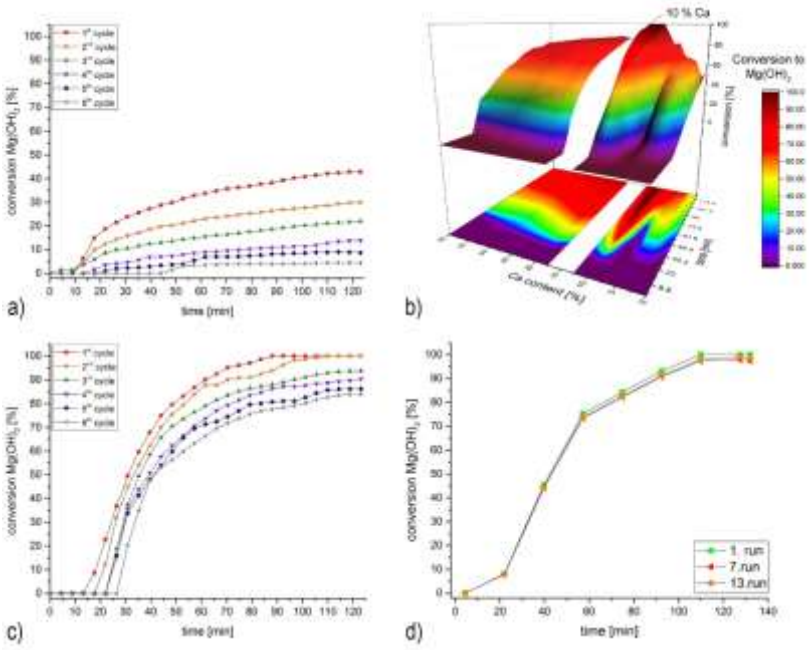

Fig. 4: Rehydration rate and cycle stability of various $Mg_{1-x}Ca_xO$ samples. a) Commercial MgO as reference. b) Comparison of $Mg_{1-x}Ca_xO$ with Ca^{2+} content between 0% and 40% (the 3D plot compares the final conversion of the different samples, whereas the contour plot at the bottom directs the focus on the reaction rate/initial delay). c) $Mg_{0.9}Ca_{0.1}O$ d) Hydration rate of $Mg_{0.9}Ca_{0.1}O$ to $Mg_{0.9}Ca_{0.1}(OH)_2$ for two consecutive cycles before and after 1st and 2nd regeneration in liquid water

4. Summary

It was demonstrated that doping MgO with Ca^{2+} by calcination of the co-precipitated mixed $Mg_{1-x}Ca_x(OH)_2$ species, the kinetic barrier to the water dissociation step of MgO rehydration could be significantly reduced. The maximum rehydration rate and cycle stability were dramatically increased for MgO doped with 10 % Ca^{2+}, $Mg_{0.9}Ca_{0.1}O$, enabling full conversion to the corresponding hydroxide within 80 minutes. The decrease in rehydration reactivity during the following cycles was attributed to agglomeration of material during the consecutive calcination / rehydration steps, impeding the access to the reactive surface. Rehydration of the less reactive material in liquid water regenerates the initial reactivity due to degradation of the aggregates. DFT calculations demonstrated the effect of the Ca^{2+} doping as both electronic and steric in nature. Expanding the lattice-constants of an MgO (001)-surface towards the values of a corresponding CaO surface results in a more stable water adsorption together with

an increased tendency toward water dissociation (size effect), whereas exchange of Mg^{2+} atoms with Ca^{2+} lowers this energy even further (electronic effect).

5. References

Müller et al., "Calcium doping facilitates water dissociation in magnesium oxide." Advanced Sustainable Systems 2.1 (2018): 1700096.

1.4.2.5.3 *TCM type: chemical reaction*

1. Introdution

The carbonation behavior of PbO was studied via PXRD at a CO_2 pressure of 2-8 bar as well as temperature regime of 25-500 °C.

2. Preparation of materials and/or supplier

$PbCO_3$ was decomposed in an electric tube furnace at 375 °C for 4 hours under constant argon (0.2 L min−1) flow to obtain a very reactive PbO sample.

3. Results

Material: lead oxide (Fig. 5a)

Chemical formula: PbO

Reactive gas: CO_2

One of the first experiments was an isobaric heating reaction from 25° to 500°C at 8 bar CO_2 with a permanent CO_2 flow passing the reaction chamber. During heating carbonation of PbO phase occurs above 240 °C, forming shannonite, a mixed 1:1 carbonate-oxide phase with a composition of $PbCO_3$·PbO. Above 340 °C parallel to the shannonite-phase a second carbonate-oxide phase with the composition $PbCO_3$·2PbO forms. Above 400 °C the shannonite-phase is decomposed, resulting in pure $PbCO_3$·2PbO phase. During slow cooling to 50 °C under 8 bar CO_2 the composition of the sample remains unchanged.

The carbonation of PbO also results in these intermediates before reaching $PbCO_3$. As $PbCO_3$ is not detected during the reaction this suggests that either increased CO_2-pressures or higher temperatures might produce pure $PbCO_3$. In a second step an isothermal storage cycle, triggered by a change in CO_2 pressure was developed. Treating PbO at 500 °C with 8 bar CO_2 results in rapid conversion of PbO to the mixed carbonate-oxide $PbCO_3$·2PbO. Once the CO_2 pressure is decreased to 2 bar, the $PbCO_3$·2PbO phase decomposes, regenerating PbO (Fig 5b).

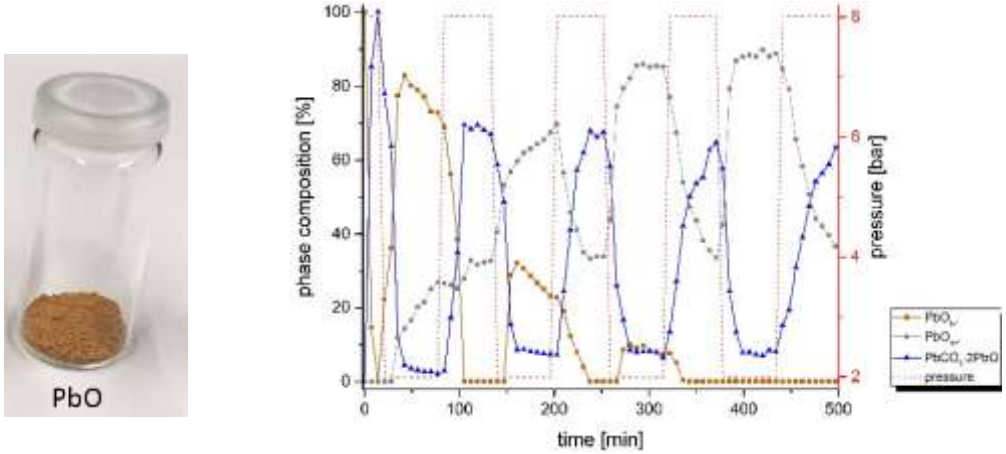

Fig. 5a: raw material (PbO); Fig. 5b: isothermal storage cycle at 500 °C between $PbCO_3$·2PbO and PbO triggered by a change in CO_2 pressure from 8 to 2 bar

4. Summary

Carbonatization of metal oxides offers a dual advantage, allowing to capture CO_2 and at the same time store thermal energy by means of a thermochemical storage cycle. For CoO, MnO, PbO and ZnO the reactivity towards CO_2 in

the presence / absence of moisture for pressures between 8-50 bar and temperatures between 25-500 °C was investigated. Isobaric heating of PbO to 500 °C at 8 bar CO_2 results in a mixed carbonate-oxide phase ($PbCO_3$·PbO) above 240 °C. Above 340 °C $PbCO_3$·2PbO a second carbonate-oxide phase starts to form. Furthermore an isothermal storage was developped. By changing the CO_2 pressure from 8 to 2 bar a cycle between the two phases $PbCO_3$·2PbO and PbO and can be triggered.

5. References

Gravogl et al., "Pressure effects on the carbonation of MeO (Me= Co, Mn, Pb, Zn) for thermochemical energy storage." Applied Energy 252 (2019): 113451.

1.4.2.6 Technical University München – Institute for Energy Systems

Dr. Annelies Vandersickel

1.4.2.6.1 *TCM type: chemical reaction*

1. Introduction:

AIM: Development of cost-effective large scale (MWh/GW) & long term energy storage for high temperature applications (300-700°C) CaO + H_2O ←→ $Ca(OH)_2$ + 104 kJ/mol

APPROACH: To exploit the low cost of the material (~ 15ct/kg), a separation of storage power (with its associated high cost for heat exchange and reactor design) and storage capacity is strived for. This is achieved using a continuously operated fluidised bed reactor. The key material requirement is therefore: good particle stability & high heat transfer in (kinetics are not limiting)

2. Preparation of materials and/or supplier

- technical grade $CaCO_3$ ((Kohlensaurer Kalk, 0.09-1.0 mm) by Märker-Gruppe GmbH
- sieved with a tumbler screening machine (TSM1200, Allgaier Process Technology) to 280-450 µm
- calcination in pure nitrogen at 800 °C for 10 min

3. Results:

a. Structural properties for porous materials and composites / formula

- Molecular Weigth: CaO = 56,08 g/mol / $Ca(OH)_2$ = 74,1 g/mol
- Bulk density: CaO = 738 kg/m³ / $Ca(OH)_2$ = 835,5 kg/m³ - declining over multiple cycles depending on operating conditions
- Specific Heat Capacity (at 25 /400°C): 0,75 / 0,91 kJ/kg K - 1,18 /1,48 kJ/kg K [2]

b. Sorption properties / reaction

- Reaction enthalpy @ 100°C:
  $CaO(s)+H_2O(liquid\ bzw.gas) \rightarrow Ca(OH)_2\ (s)+(\Delta HR \cong -67$ resp.$-108\ kJ/mol)$

c. Thermochemical properties

Reaction enthalpy @ 500°C (steam/gas): 100,5 kJ/mol

in kJ/mol		in %	
Reaction enthalpy ΔHR	100,46		100,00
Evaporation enthalpy	40,67		40,48
Chemically stored energy	59,79		59,52

d. Picture/image/photograph of the material: Lichtmikroscopie

Source [1]

→ Reaction enthalpy @ 100°C:
CaO(s)+H_2O($l$iquid $bzw.g$as) →Ca($OH)_2$ (s)+(ΔHR≅−67 resp.−108 kJ/mol)

Reaction enthalpy @ 500°C (steam/gas): 100,5 kJ/mol

	in kJ/mol	in %
Reaction enthalpy ΔHR	100,46	100,00
Evaporation enthalpy	40,67	40,48
Chemically stored energy	59,79	59,52

Source: [1]

4. Summary

Very fast kinetics in pure steam atmosphere over a wide range of H2O pressure (1.5 till 3 bar).

5. References

[1] Moritz Becker, Thermochemische Energiespeicherung Mit Calcium-Oxid Und -Hydroxid: Entwicklung Eines Reaktorkonzeptes, Dissertation, Technical University Munich, Institute for Energy Systems (submitted)
[2] CHASE, Malcolm: *NIST-JANAF Thermochemical Tables, 4th Edition* : American Institute of Physics, 1998 (NIST-JANAF Thermochemical Tables, 4th Edition)
[3] M. Angerer, M. Becker, S. Härzschel, K. Kröper, S. Gleis, A. Vandersickel, H. Spliethoff, Design of a MW-scale thermo-chemical energy storage reactor, Energy Reports **4** (2018) 507-519.

1.4.2.7 The Netherlands organization for Applied Scientific Research TNO – department of sustainable process & energy systems (SPES)

Dr. Ruud Cuypers

1.4.2.7.1 *TCM type: chemical reaction*

1. Introduction:

Newly developed salt hydrate materials made of sodium sulphide (Na_2S) with different percentages of enhancing additives are used as heat storage medium for closed-sorption (vacuum) compact heat batteries for dwellings (heating, domestic hot water), for charging up to 80°C, and discharging up to 65°C.

2. Preparation of materials and/or supplier:

Samples were synthesized by mixing/melting and co-crystallization of pure materials to form scales/powder. Materials are separated into different sieve fractions. Pellets can be prepared should this be desired.

3. Results

Materials are used in several different analyses to investigate pT-diagrams and sorption behavior, kinetics, outgassing behavior, cycling behavior, all as single-layers and as packed-beds. In addition, materials are tested in a mock-up heat battery under relevant testing conditions to investigate power and heat storage capacity.

a. Structural properties for porous materials and composites / formula

Materials are present as scales and/or as pellets, with typical dimensions of 1-6mm length and 1-2mm thickness, depending on the sieve fractions used.

b. Sorption properties / reaction

Materials can exist as anhydrate, hemihydrate, dihydrate, pentahydrate and nonahydrate. The utilized reactions proceeds from hemihydrate to pentahydrate and vice versa and goes as follows:

$Na_2S.5H_2O$ (s) ↔ $Na_2S.0.5H_2O$ (s) + $4.5H_2O$ (g) $\Delta H^0 = \pm$ 283 kJ/mol $Na_2S.5H_2O$

Below, a typical result for multiple hydration / dehydration cycles of single layers (solid lines) and packed bed (dashed lines) of several sieve fractions of materials is given with mass fraction reacted as a function of time in hours (logarithmic).

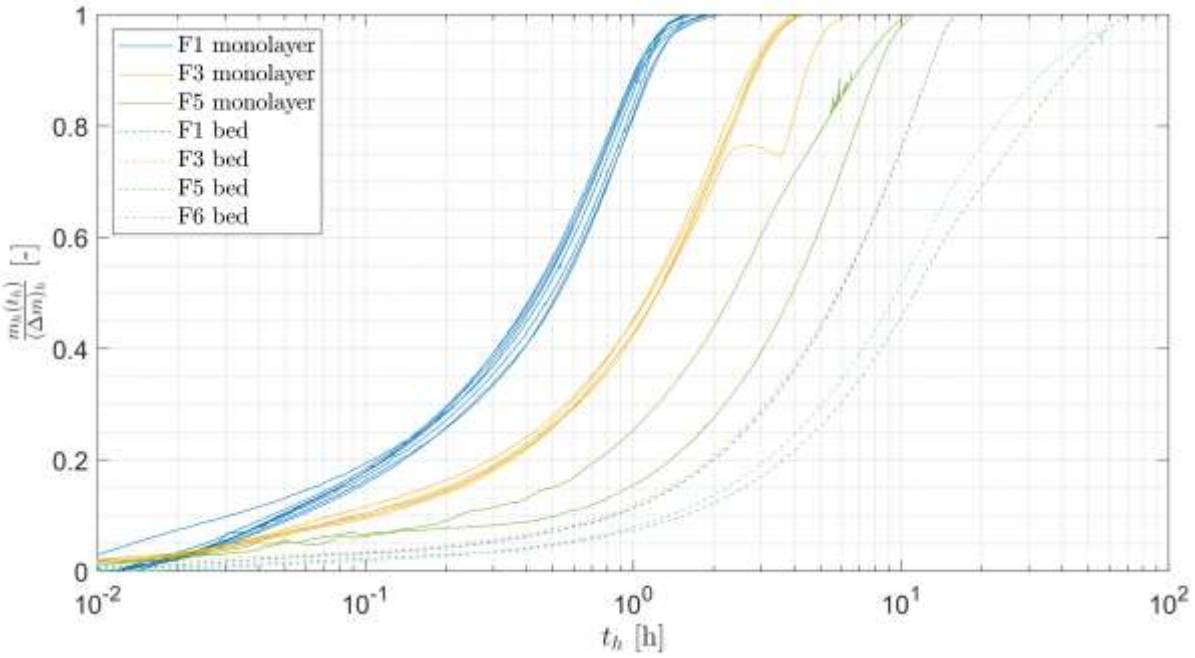

c. Thermochemical properties:

The performances of the synthesized materials were evaluated by thermogravimetric analysis, which simulates the use in the closed-sorption heat battery. A storage density of 1.5 GJ/m^3 (based on pentahydrate density of 1580 kg/m^3 and co-storage of 0.76 m^3 water per m^3 pentahydrate) was calculated (validation in a heat battery still to be done).

d. Picture/image/photograph of the material:

e. Graph:

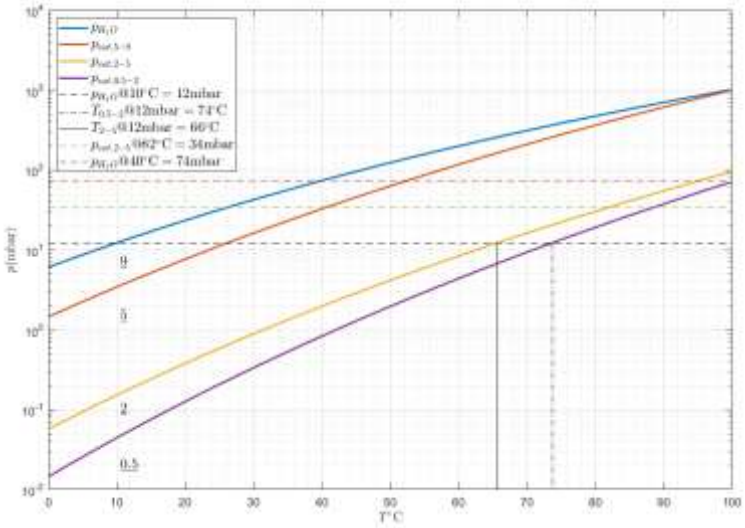

4. Summary :

As main results it is found that i) materials can be cycled between charged and discharged state without noticeable deterioration as a function of the number of cycles; ii) monolayers of smaller particles charge and discharge much faster than those of larger particles; iii) heat and mass transfer inside these particles is described, but still under further investigation.

5. Reference

"Preparation & characterization of sodium sulfide hydrates for application in thermochemical storage systems", M. Roelands, R. Cuypers, K. Kruit, H. Oversloot, A.J. de Jong, H. van 't Spijker, W. Duvalois, L. van Vliet, C. Hoegaerts, Energy Procedia, 2015, 70, 257 – 266.

1.4.3 Overview of TCM materials

Some of data for sorption couples and chemical reactions are selected and summarized in Figures 1 and 2, respectively, to give an overview of relations between energy storage capacities or reaction enthalpies and desorption / reaction temperatures. The data listed in Figure 1 are based on experiment results (4T approach), while Figure 2 contains theoretical calculations. The data were provided by: University Messina and CNR-ITAE Messina Italy, National Institute of Chemistry Slovenia, CanmetEnergy Ottawa and Simon Fraser University, Canada, CIC Energigune Spain, TU Wien Austria, Materials Science & Eng. Department Northwestern University, USA and Institute of Catalysis and Petrochemistry, Madrid, Spain.

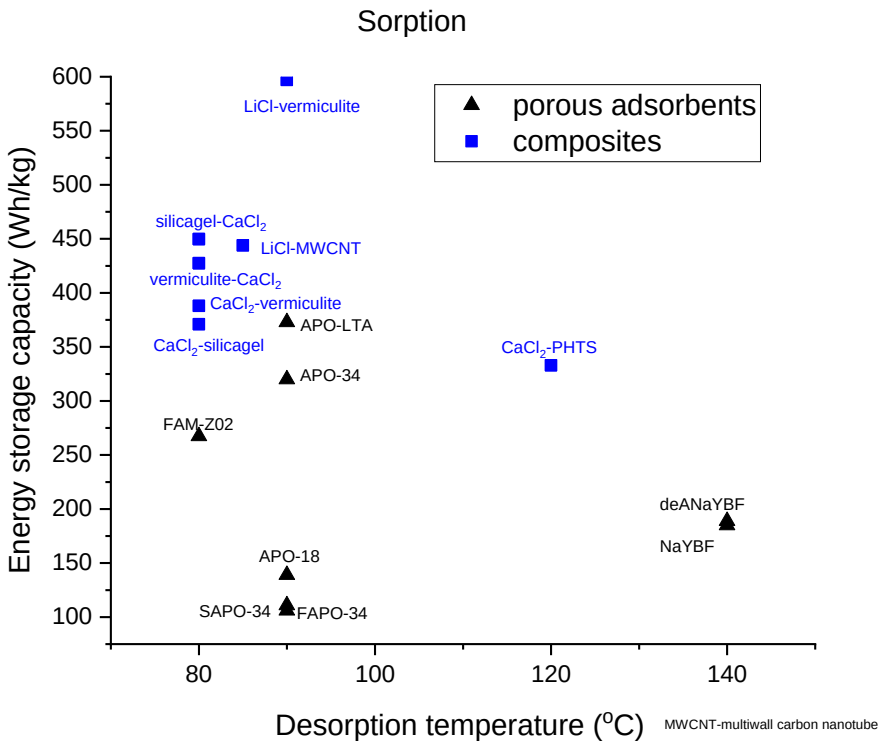

Figure 1: Energy storage capacity versus a desorption temperature of porous solids and composites (adsorbate water) investigated between 2017-2019 for sorption heat storage

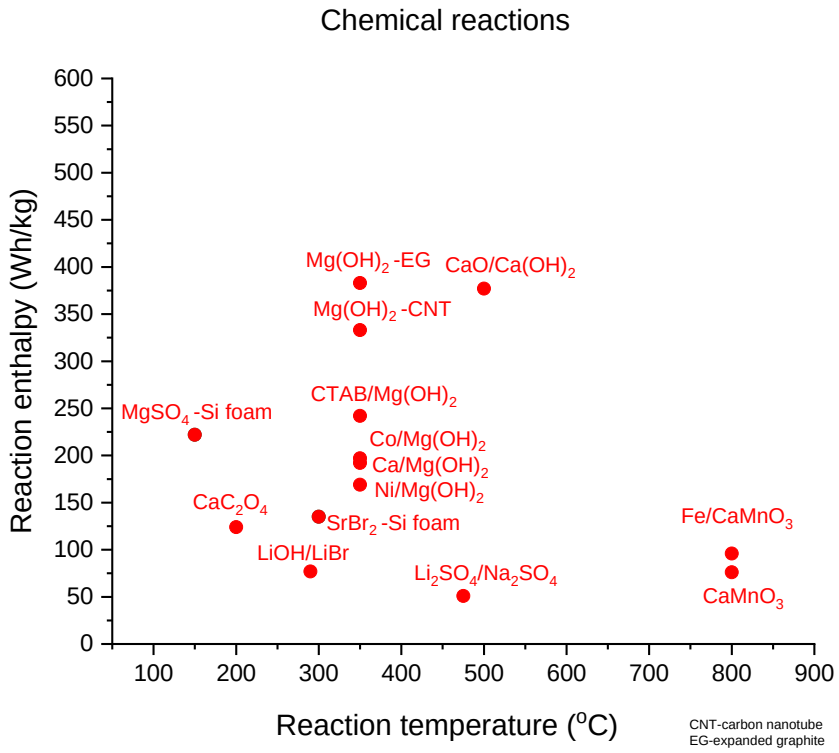

Figure 2: Reaction enthalpies of oxides and composites versus reaction temperature for different TCMs

1.5 Developement of the TCM material databases implemented in Task42/Annex 29

Due to complexicity and different relevant materials` properties it was decided to prepare three databases: one on chemical reactions (salt hydrates, oxides, composites), one on adsorption (porous solids and composites) and one on absorption (liquids). Materials parameters were determined for the first two databases (see section a in b) and are similar, while the third one is completely different and much more complex. As such it cannot be incorporated in the present frame for chemical reactions and sorption materials.

1.5.1 Material parameters for the chemical reaction database using K_2CO_3*1.5 H_2O as an example:

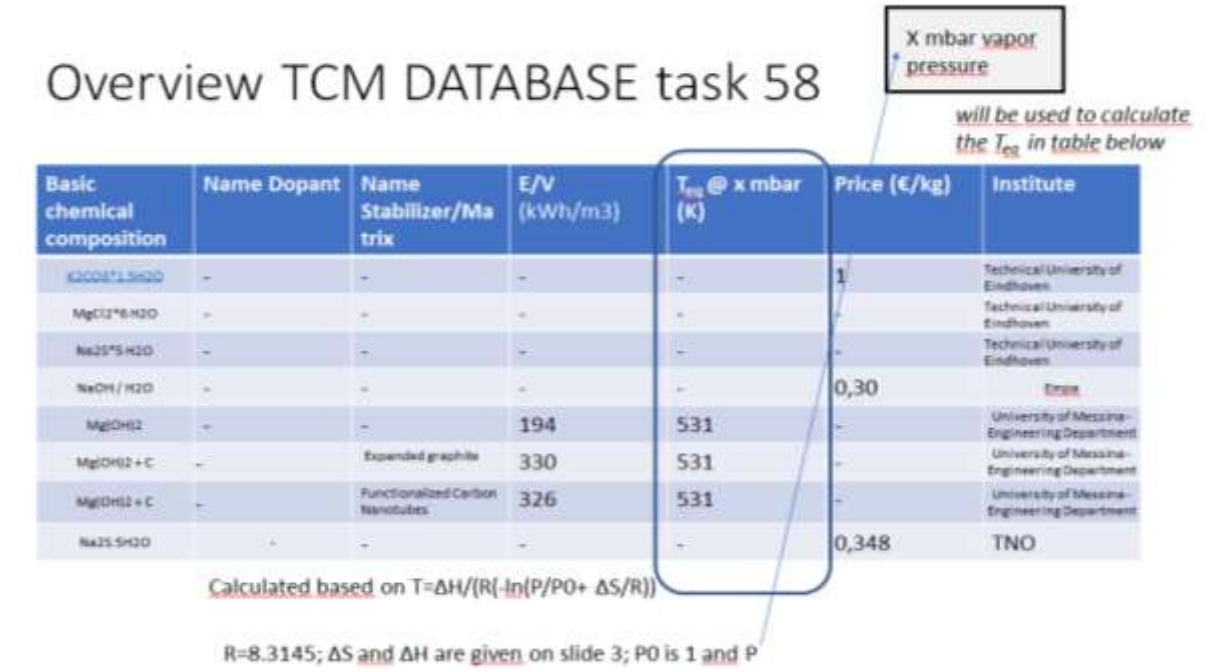

Basic chemical composition	Name Dopant	Name Stabilizer/Matrix	E/V (kWh/m3)	T_{eq} @ x mbar (K)	Price (€/kg)	Institute
K2CO3*1.5H2O	-	-	-	-	1	Technical University of Eindhoven
MgCl2*6 H2O	-	-	-	-	-	Technical University of Eindhoven
Na2S*5 H2O	-	-	-	-	-	Technical University of Eindhoven
NaOH / H2O	-	-	-	-	0,30	Empa
Mg(OH)2	-	-	194	531	-	University of Messina - Engineering Department
Mg(OH)2 + C	-	Expanded graphite	330	531	-	University of Messina - Engineering Department
Mg(OH)2 + C	-	Functionalized Carbon Nanotubes	326	531	-	University of Messina - Engineering Department
Na2S.5H2O	-	-	-	-	0,348	TNO

Back to TCM overview

Basic chemical composition : K2CO3*1.5H2O

Starting Materials properties
Reaction data
Testing conditions and performance
Cyclability and effect on the material
Additional information
Back to TCM overview

Reaction data	*Number of transitions*		*1*
	Equilibrium reaction (aA+bB4→cC+heat)	Type of reaction	hydration
	Name A		K2CO3
	state of A	Gas/Liquid/Solid	Solid
	a		1
	Molar Mass A	g/mol	138
	Melting point A	K	?
	Specific density A	kg/m³	
	Specific heat capacity A	J/(g K)	
	Deliquescence point a (at 25 °C)	Mbar	
	Name B		H2O
	state of B	Gas/Liquid/Solid	Gas
	b		1,5
	Molar Mass B	g/mol	18,02
	Specific density B	kg/m³	
	Melting point B	K	nyt
	Specific heat capacity B	J/(g K)	
	Deliquescence point B (at 25 °C)	Mbar	
	Name C		K2CO3·1.5H2O
	State of C	Gas/Liquid/Solid	
	c		1
	Molar Mass c	g/mol	165
	Specific density C	kg/m³	
	Melting point c	K	?
	Specific heat capacity C	J/(g K)	
	Deliquescence point c (at 25 °C)	mbar	
	ΔS° (standard entropy of the equilibrium reaction)	J/(mol·K)	151
	ΔH° (standard ethalpy of the equilibrium reaction)	kJ/mol	62.5
	Teq = ΔH°/ΔS°	K	
	pT diagram	link to referene	
	Theoretical energy density	kJ/kg	
	Deliquescence line	Link to reference	

Basic chemical composition : K2CO3*1.5H2O

Starting Materials properties
Reaction data
Testing conditions and performance
Cyclability and effect on the material
Additional information
Back to TCM overview

Material properties under testing conditions	Apparent (bulk) heat conductivity (charged state; A)	(W/(m·K))	
	Specific heat conductivity single grain (charged state; A)	(W/(m·K))	
	Apparent (bulk) heat conductivity (discharged state; C)	(W/(m·K))	
	Specific heat conductivity single grain (discharged state; C)	(W/(m·K))	
	Reference		
Testing conditions and performance			
	instrument used for testing (i.e. TGA, lab scale reactor,..)		TGA
	Charging conditions - energy stored in TCM	Test cell volume (cm3)	
		Starting temperature (K)	80
		Final temperature (K)	70
		heating rate (K/min)	0.5
		Type of gas	air
		Total flow rate (ml/min)	500
		Total flow speed at reactor/sample (m/s)	-
		Total pressure (mbar)	1000
		Mass flow solid phase (g/s)	0
		Residence time in reactor of solid material (s)	n/a
		partial pressure reactive gas (mbar)	7.3
		Time (min)	31.3
		initial sample mass (g)	0.006196
		Mass variation (g)	0.000079
	Discharging conditions - energy released by TCM	Starting temperature (K)	80
		Final temperature (K)	25
		heating rate (K/min)	-0.5
		Type of gas	air, N2
		Total flow rate (ml/min)	500
		Total pressure (mbar)	1000
		Total flow speed at reactor/sample (m/s)	-
		Mass flow solid phase (g/s)	0
		Residence time in reactor of solid material (s)	n/a
		partial pressure reactive gas (mbar)	7.3
		Time (min)	92.3
		initial sample mass (g)	0.00821
		Method of determination mass variation	TGA
		Mass variation (g)	0.001349
	Charging power (W/g) - peak	W/g	
	Mean charging power (W/g) - based on complete charging period	W/g	
	Discharging power (W/g)	W/g	
	Mean discharging power (W/g) - based on complete discharging period	W/g	
	Experimental Charging efficiency	ratio/kg	
	Experimental Released efficiency	ratio/kg	
	Experimental Storage Energy Density	(kWh/m3)	
	Experimental Released Energy Density	(kWh/m3)	
	Diagram of the experiment	picture	
	Reference of kinetic study of described reaction		

Basic chemical composition : K2CO3*1.5H2O

Starting Materials properties
Reaction data
Testing conditions and performance
Cyclability and effect on the material
Additional information

Cyclability and effect on the material	Number of cycles studied	%	9
	Storage Efficiency at n cycle (η=Storage Energy Density at n cycle/ Storage Energy Density at 1st cycle)	nm	1
	Mean particle size of grains(nm) after n^{th} cycle	µm	
	Mean primary crystallite size(µm) after n^{th} cycle		
	Picture of the particles (before/during/after experiment)		
	Diagram of the experiment		
	Reference to experiment	N	
	Crushing strength Starting material	N	
	Crushing strength after n^{th}	%	

Back to TCM overview

Basic chemical composition : K2CO3*1.5H2O

Starting Materials properties
Reaction data
Testing conditions and performance
Cyclability and effect on the material
Additional information

Additional Information	Price (euro/kg, euro/MJ)	(euro/kg)	1
		Supplier	not
		(euro/MJ)	
	Safety	Link to MSDS data	
	Corrosion	Link to corrosion data	
	References	General references about this material/reaction/...	G. P. Thiel and J. H. Lienhard, Desalination, vol. 346, pp. 54–69, Aug 2014

1.5.2 Material parameters for the sorption materials database

Materials properties	Materials properties	Adsorbent material		Zeolite 13X	Text
		Supplier		Chemiewerk Bad Köstritz, Germany	Text
Testing conditions and performance		Sample conditions	Powder, granulated, extruded...	granulated beads, binder-free, diameter: 1.6–2.5 mm	Text
Cyclability and effect on the material		Synthesis route		REFERENCE reported in the reference section	Text
		Adsorbate		Water	Text
		Gas carrier	If any	Air	Text
Additional Information		Adsorbent density	bulk, crystallographic, fixed bed	680 kg/m^3 - bulk	Integer + text
		Density source	from "measurements", "literature" or the material "supplier"	REFERENCE reported in the reference section	Text
		Density Measurement Temperature		25°C	Integer

1.6 Acknowledgements

Financial support from the Slovenian Research Agency through the research program P1-0021 (Nanoporous materials) and the research project L1-7665 (Advanced heat storage materials for integrated storage solutions) is acknowledged.

The project has received funding from the European Union's Horizon 2020 research and innovation programme under the Marie Sklodowska-Curie grant agreement N° 74616. Support of the US Department of Energy, Office of Energy Efficiency and Renewable Energy, Award DE-EE0008089.0000, is also acknowledged.

The research was funded by the European Union's Horizon 2020 research and innovation program under the Marie Skłodowska-Curie grant agreement No 752520". SOLSTORE project (*Solid-state reactions for thermal energy storage*).

The Austrian Research Promotion Agency FFG within the project SolidHeat Pressure (#853.593) is thanked for financial support.

The project "Thermochemical materials for heat storage: development and characterization" has been sponsored by INSTM (Consorzio Interuniversitario Nazionale per la Scienza e Tecnologia dei Materiali, grant number INSTMME002).

Nordforsk, Norway and KTH Royal Institute of Technology, Sweden for financing the Neutrons for heat storage (NHS) project are acknowledged.

The Dutch ministry of Economic Affairs, Energy in the Built Environment, Project Nr. 060.37230 is acknowledged.

Financial support for project New-TCM (Wi-2018-97351/9-RA) by the EU-European Regional Development Fund (ERDF) and Federal Province of Upper Austria- Investments in Growth and Jobs (IGJ) is gratefully acknowledged.